

MICROCOPY RESOLUTION TEST CHART
NATIONAL BUREAU OF STANDARDS-1963-A

12

SACLANTCEN Report SR - 104
SACLANTCEN Report SR - 104

DTIC FILE COPY

SACLANTCEN Report SR - 104

**SACLANT ASW
RESEARCH CENTRE
REPORT**



AD-A179 060

**HIGH-RESOLUTION BEAMFORMING TECHNIQUES
PERFORMANCE ANALYSIS**

by
Walter M. X. ZIMMER

NOVEMBER 1986

DTIC ELECTED
S D
APR 09 1987
E

NORTH
ATLANTIC
TREATY
ORGANIZATION

SACLANTCEN
LA SPEZIA, ITALY

This document is unclassified. The information it contains is published subject to the conditions of the legend printed on the inside cover. Short quotations from it may be made in other publications if credit is given to the author(s). Except for working copies for research purposes or for use in official NATO publications, reproduction requires the authorization of the Director of SACLANTCEN.

This document has been approved for public release and only its distribution is unlimited.

87 4 7 - 196

This document is released to a NATO Government at the direction of the SACLANTCEN subject to the following conditions:

1. The recipient NATO Government agrees to use its best endeavours to ensure that the information herein disclosed, whether or not it bears a security classification, is not dealt with in any manner (a) contrary to the intent of the provisions of the Charter of the Centre, or (b) prejudicial to the rights of the owner thereof to obtain patent, copyright, or other like statutory protection therefor.

2. If the technical information was originally released to the Centre by a NATO Government subject to restrictions clearly marked on this document, the recipient NATO Government agrees to use its best endeavours to abide by the terms of the restrictions so imposed by the releasing Government.

NORTH ATLANTIC TREATY ORGANIZATION

SACLANT ASW Research Centre
Viale San Bartolomeo 400,
I-19026 San Bartolomeo (SP), Italy.

tel: national 0187 540111
international + 39 187 540111

telex: 271148 SACENT I

(12)

SACLANTCEN SR-104

HIGH-RESOLUTION BEAMFORMING TECHNIQUES PERFORMANCE ANALYSIS

by
Walter M.X. Zimmer

November 1986

Accession For	
NTIS GRA&I	<input checked="" type="checkbox"/>
DTIC TAB	<input type="checkbox"/>
Unannounced	<input type="checkbox"/>
Justification	
By _____	
Distribution/	
Availability Codes	
Dist	Avail and/or Special
A-1	

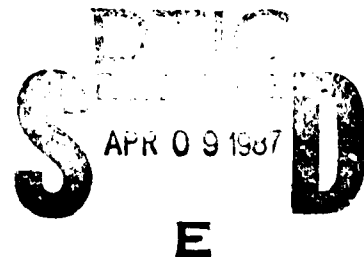


This report has been prepared as part of Project 02.
Date of submission: 20 Dec 1985

Approved for Distribution

Ralph R. Goodman

Ralph R. Goodman
Director



This document has been approved
for public release and sale; its
distribution is unlimited.

CONTENTS

ABSTRACT	1
INTRODUCTION	2
1 DESCRIPTION OF THE PROBLEM	2
1.1 General problem formulation	2
1.2 Comments on the beamformer output	4
2 PRESENTATION OF THE BEAMFORMING TECHNIQUES	5
2.1 Estimation of the correlation function	5
2.2 Conventional Beamforming	7
2.3 Adaptive Beamforming	8
2.4 Maximum Entropy Beamforming	9
2.5 Orthogonal Beamforming	11
3 THEORETICAL RESULTS	14
3.1 Summary of the beamforming techniques	14
3.2 Conventional Beamforming	15
3.3 Adaptive Beamforming	16
3.4 Maximum Entropy Beamforming	16
3.5 Orthogonal Beamforming	16
4 DETECTION PERFORMANCE	21
4.1 Preliminaries	21
4.2 Detection probability	22
4.3 Accuracy of the bearing estimation	22
5 RESOLUTION PERFORMANCE	26
5.1 Scenario	26
5.2 Resolution probability	26
6 SUMMARY	28
REFERENCES	30
APPENDIX A - Further comments on the beamformer output	31
APPENDIX B - Summary of single source simulations	32
APPENDIX C - Summary of two source simulations	42

**HIGH-RESOLUTION BEAMFORMING TECHNIQUES
PERFORMANCE ANALYSIS**

by
Walter M.X. Zimmer

ABSTRACT

Seven different beamforming techniques (including both conventional and high-resolution types) have been analyzed and compared in order to develop a quantitative relationship between resolution performance on the one hand and detection and the accuracy of bearing estimation on the other. The techniques discussed are the Blackman-Tukey Conventional, the Wiener Conventional, the Capon Adaptive and the Maximum Entropy Beamformers, and the Optimal, the Johnson, and the Schmidt Eigenvector Methods. Detection performance, accuracy, and resolution of the different techniques are discussed and tabulated.

Walter M.X. Zimmer

INTRODUCTION

The resolution performance of conventional beamforming techniques is limited by the length of the array (i.e. the array aperture). Therefore high-resolution beamforming techniques may be achieved only by extrapolating the measurements (or some function of them) beyond this array aperture. From mathematics we know that extrapolations work reliably only in the absence of measurement errors or noise. In real life, however, noise-free measurements are not possible. The detection problem is characterized by a low signal-to-noise ratio, i.e. noise dominates the measurements and the signal is barely detectable. Also, the accuracy of source bearing estimation is influenced by noise. Therefore any extrapolation of the measurements beyond the array aperture will likely degrade the detection performance of the beamformer and also the accuracy of the source bearing estimation. The main purpose of this report is to analyze and compare several different beamforming techniques in order to develop a more quantitative relation between resolution performance on the one hand and detection performance and accuracy of bearing estimation on the other.

1. DESCRIPTION OF THE PROBLEM

1.1 General problem formulation

Figure 1 sketches the following scenario: an array of hydrophones receives sound from two point sources that are assumed to be at an extreme distance to avoid complications due to changing geometry. This is equivalent to assuming constant bearing of the two sources from the array. The measured data are processed with some particular beamforming method and the output is then displayed.

Figure 1 shows the theoretical result of both a conventional and a high-resolution method. The conventional technique is characterized by broad main lobes in source direction and more or less marked sidelobes. The significant features of the high-resolution method are the sharp peak in source direction and the increased difference between the peak maximum and the mean noise level. Three questions arise concerning the performance of this high-resolution method:

- Do narrow peaks indicate better resolution performance?
- Is the bearing estimate more accurate?
- Do increased peak-to-noise ratios indicate better detection performance?

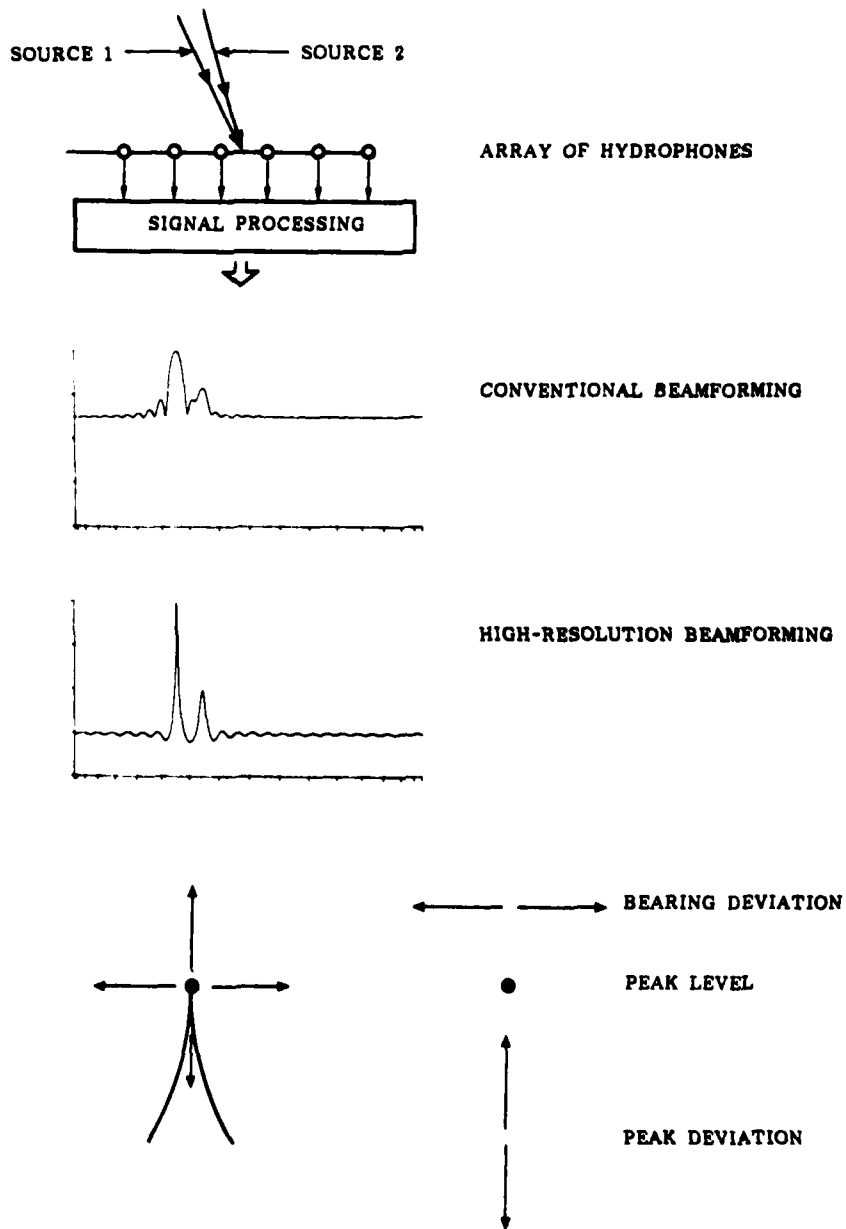


Fig. 1: Problem formulation; statistical analysis of passive sonar signal processing.

In an attempt to answer these questions, numerous computer simulations were made. The analysis of these simulations has focused on

- the distribution of the estimated peak level which yields the detection performance.
- the distribution of the estimated source bearing which results in the resolution performance and the accuracy of source bearing estimation.

In detail, we will see how the peak-level statistic varies as a function of input signal-to-noise ratio. Further, we will see the degree of uncertainty in bearing estimation, measured as a function of input signal-to-noise ratio and as a function of the separation from a second, closely-spaced source.

1.2 Comments on the beamformer output.

When using a beamformer, we will assume that we wish to measure the spatial power distribution. For such a case we apply the Wiener-Khinchin theorem and represent the power spectrum as the Fourier transform of the spatial correlation function, thus:

$$P(f) = \sum_{k=-\infty}^{\infty} r_k e^{-2\pi i k f}, \quad -\frac{1}{2} \leq f \leq \frac{1}{2}. \quad \text{Eq.(1)}$$

If we know the entire correlation function, that is, knowing r_k for all values of k , then we can obtain the power spectrum by means of Eq.1. However, in many applications, we know (or can reliably measure) the correlation function only for a certain finite number of k values, say for $-p \leq k \leq p$, and thus we do not know the value of r for $|k| > p$.

To estimate the power spectrum from this partial knowledge we either

- ignore the long range correlation which yields the class of conventional beamformer,
- or extrapolate the correlation function beyond the array aperture to define the class of high-resolution beamformer [1].

2. PRESENTATION OF THE BEAMFORMING TECHNIQUES

In the following chapter seven different techniques for beamforming will be presented. The techniques can be conveniently classified into four different groups:

- a. Conventional Beamforming :
 - Blackman-Tukey method
 - Wiener method
- b. Adaptive Beamforming:
 - Capon method
- c. Maximum Entropy Beamforming:
 - Forward-Backward Linear Predictor
- d. Orthogonal Beamforming
 - Optimal Eigenvector method
 - Johnson Eigenvector method
 - Schmidt Eigenvector method

2.1 Estimation of the correlation function.

To begin we must first say some words about the spatial correlation function and its estimation. According to the Wiener-Khinchin theorem the correlation function plays an important part in spectral analysis. The same observation is also valid in spatial beamforming.

For a wide sense stationary process the (spatial) correlation function is defined by

$$r_k = \lim_{M \rightarrow \infty} \frac{1}{2M - |k|} \text{Tr}(\Omega^k \langle yy^* \rangle),$$

where

Ω is the next neighbour difference matrix with dimension (M, M) ,

$$\Omega_{i,j} = \rho(i - j = 1),$$

$$\Omega^{-1} = \Omega^T,$$

y is the measurement vector of dimension M ,

$\langle \dots \rangle$ is the statistical average, and

$$\rho(i - j = 1) = \begin{cases} 1, & \text{if } i - j = 1; \\ 0, & \text{otherwise.} \end{cases}$$

Unfortunately there is no possibility of getting the true correlation function from real

measurements as this would need infinite spatial and statistical averages. However, we can provide a more or less reliable estimate of the correlation function. Because this estimate is always erroneous the power estimate cannot be the true one. It is important to realize that the power estimate can be only as accurate as the estimate of the correlation function.

The major restriction is that we cannot perform an infinite spatial average (i.e. $M \rightarrow \infty$). This restriction leads to two consequences:

- for a spatially wide-sense stationary random process the estimate of the correlation function will be noisy.
- because the maximal correlation lag is limited by the array aperture we cannot estimate long range correlation.

If we drop the notation $M \rightarrow \infty$, the unbiased estimate of the correlation function is given by

$$\hat{r}_k = \frac{1}{2M - |k|} \text{Tr}(\Omega^k \langle yy^* \rangle). \quad \text{Eq.(2)}$$

The next problem is to compute the statistical average. In the case of beamforming it is convenient to replace the statistical average by a time average. This is justified when the sound field is weakly stationary, not only in space, but also in time. Then we can write

$$\langle \dots \rangle = \frac{1}{T} \sum_{t=1}^T \dots$$

Further statistical averaging can be performed by replacing the data vector in Eq.(2) by a forward-backward data matrix

$$\begin{pmatrix} y_1 \\ \vdots \\ y_M \end{pmatrix} \mapsto \frac{1}{\sqrt{2}} \begin{pmatrix} y_1, & y_M^* \\ \vdots & \vdots \\ y_M, & y_1^* \end{pmatrix}.$$

The effect of this is to replace $\langle yy^* \rangle$ by the average between the usual forward correlation matrix and the backward correlation matrix that would result by using the "backward" data vector.

The reason for this procedure is explained by the following observation:

If y_n represents a wide sense stationary process, then its direction-transposed conjugated image will also be wide sense stationary with identical correlation function. Therefore the forward-backward average increases the estimation accuracy of the correlation function [2].

2.2 Conventional Beamforming

Conventional beamforming is characterized by the fact that the long range correlation is ignored completely or, equivalently, it is assumed to be zero, thus

$$\hat{r}_k = 0, \quad |k| > p.$$

Therefore the power spectrum estimate results in

$$\hat{P}(f) = \sum_{k=-p}^p \hat{r}_k e^{-2\pi i k f}.$$

There are two main approaches to estimate the correlation function:

- the Blackman-Tukey approach uses the unbiased finite estimate of the correlation function given in Eq.(2).

$$\hat{r}_k = r_k, \quad |k| \leq p.$$

The finite aperture of the array acts like a rectangular window on the correlation function. Therefore the true power spectrum can be achieved for short range correlated processes (i.e. wide angle noise), but the spectrum is heavily oscillating in situations where the long range tail of the correlation function is of importance (point sources).

- The Wiener approach reduces these oscillations and always ensures positive power estimates by using a biased estimate of the correlation function. This estimate is given by multiplying the unbiased estimate with a triangular (Bartlett) window:

$$\hat{r}_k = \left(1 - \frac{|k|}{p}\right) r_k, \quad |k| \leq p.$$

Besides these power estimators that are based on the correlation function, we have the Periodogram Method of Schuster. This method was the first important application of the Fourier Spectral Theorem. In this method the power spectrum is defined as the squared value of the Fourier Transform of all the data:

$$\hat{P}(f) = \left| \sum_{n=1}^M y_n e^{-2\pi i n f} \right|^2.$$

It is easy to see that this method transforms to the Wiener approach by taking the expectation value on both sides

It should be noted that the expression, conventional beamforming, is used in a wider sense than usual. The normal usage regards only the periodogram and the Wiener approach as conventional beamformers. For systematic reasons, however, the Blackman-Tukey approach also will be called conventional because it is the unbiased implementation of the Wiener-Khinchin theorem.

2.3 Adaptive Beamforming

One of the early high-resolution methods is the adaptive beamforming technique of Capon [3]. This approach, sometimes called maximum likelihood method, extends the correlation function in such a way that interferences from all other than the steering directions become minimum. This is equivalent to minimizing the beamformer output under the constraint that the response in a given direction is kept constant.

Using the Lagrange multiplier method we can write the unconstrained optimization procedure as follows:

$$d^* S d + \mu (d^* w - c) \rightarrow \min,$$

where

- $S = \langle yy^* \rangle$ is the cross correlation matrix,
- d is the optimal steering vector,
- μ is some Lagrange parameter,
- $w = w(f)$ is the look direction,
- c is some constant.

The resulting power spectrum estimate is given by

$$\hat{P}(f) = \sum_{k=-N}^N \hat{r}_k e^{-2\pi i k f} \frac{1}{w^* S^{-1} w},$$

where $N \gg p$ is the desired aperture of the beamformer.

There is no known closed-form expression to show how the correlation function \hat{r}_k is estimated within and outside the physical array aperture. However, some indication for this behaviour may be found in [1]. In this report it is only of importance that the Capon method modifies the measured part of the correlation function and tries to produce a smooth extrapolation.

2.4 Maximum Entropy Beamforming

In this paragraph the maximum entropy principle will be discussed as a method yielding high resolution. This principle is well known in physics; for example it is the basis of statistical mechanics.

Before we formulate the maximum entropy principle we have to define entropy:

Entropy is a measure of the number of distinct possible ways of achieving a probability distribution.

A high value of entropy therefore means that the probability distribution has an extensive statistical support. The maximum entropy principle, a plausible consequence, says:

Inferences based on incomplete information should be drawn from whichever probability distribution has the maximum entropy permitted by the available information.

As an example, if we only have knowledge about second-order statistics the maximum entropy principle results in the gaussian probability distribution as a basis for inferences.

The maximum entropy principle produces the following consequence:

Unless there are further constraints which are not revealed in the statement of the problem, the great majority of the true power spectra will be close to the maximum entropy estimate, because the great majority of all possible spectra have that property. Conversely if the maximum entropy estimate turns out to be significantly in error, then we have statistically significant evidence for the existence of a systematic effect separating us from the desired solution.

The maximum entropy method is reliable in the sense that it cannot show any details for which there is no evidence in the data [4].

Assuming that we know the expectation value of the correlation function r (our variable of interest), then the maximum entropy is given by [4, 5]

$$H_{\max} = \log Z + \lambda^T r,$$

where

- Z is the partition function,
- r is the expectation value of the correlation function,
- λ is a vector of Lagrange parameters.

The Lagrange parameter in this equation can be interpreted simply as the potential of the corresponding data. Redundant data, which by definition do not contribute to the entropy, are at zero potential. On the other hand, highly relevant data are those without which our estimate would be very different; they have a large potential and their absence would greatly lower the entropy.

This rather abstract treatment of the maximum entropy principle was introduced to show that, theoretically, this principle is very appealing. However we will see later on that the optimal behaviour cannot be achieved in reality.

The maximum entropy spectral estimate is given by

$$\hat{P}(f) = \sum_{k=-N}^N \hat{r}_k e^{-2\pi i k f} = \left| \frac{1}{a^* w} \right|^2,$$

where $N \gg p$ is the desired aperture of the beamformer and the vector, a , may be estimated via the relation

$$a^* R a - \mu (a^* c - 1) \rightarrow \min$$

with

$$R = \sum_{k=-p}^p r_k \Omega^k,$$

$$c = (1, 0, \dots, 0)^T,$$

μ is some new Lagrange parameter.

The power spectrum estimate is then given by

$$\hat{P}(f) = \frac{\left| c^T R^{-1} c \right|^2}{\left| c^T R^{-1} w \right|^2}.$$

The maximum entropy spectrum is consistent with the Wiener-Khinchin theorem because it is only the closed form solution in which the unknown part of the correlation function is replaced by the estimate based on the maximum entropy signal distribution. The extrapolation of the correlation function is consistent with the data and introduces no new information into the spectrum.

However, the power spectrum estimate is optimal in the maximum entropy sense only if the correlation matrix is of Toeplitz form. In reality this may only be achieved with infinite temporal or statistical average. Therefore, any implementation of a maximum

entropy spectrum estimator will be sub-optimal and sometimes have unpredictable results. To achieve acceptable results Nuttall [2] proposed to use a forward-backward averaged estimate of the correlation matrix. A further ad hoc assumption is given by the limitation of the maximum measured correlation length to a value less than the array aperture. This results in additional statistical stability. This implementation of the maximum entropy principle is also called the forward-backward linear predictor and will be used in this report.

2.5 Orthogonal Beamforming

The orthogonal beamforming principle is based on the following observations:

- the correlation matrix is Hermitian and therefore all its eigenvectors are mutually orthogonal;
- if the correlation matrix is of rank M and the signal alone correlation matrix is of rank $K < M$, then $M - K$ noise (signal free) eigenvalues exist;
- if the noise is white and the correlation matrix exactly known, then the noise eigenvectors are orthogonal to the signal bearing vectors.
- if the correlation matrix is known but the noise is not white, then there is orthogonality between the noise eigenvectors and the signal bearing vectors obtained after the appropriate transformation (given by the spatial pre-whitening of the noise) is applied.

The fundamental eigenvector method is due to Pisarenko (e.g.[6]) and may be described as a minimum interference method, where the solution vector d is found via the constant norm optimization procedure,

$$d^* R d + \mu d^* d \rightarrow \min,$$

with the solution

$$\mu = \lambda_{\min}$$

as the minimum eigenvalue of R , and

$$d = v_{\min}$$

as the eigenvector associated with λ_{\min} (also called minimum eigenvector).

To have a beamformer output a pseudo-power estimate may be defined using a formula similar to the maximum entropy spectrum estimate:

$$\hat{P}(f) = \frac{\lambda_{\min}}{|v_{\min}^* w|^2},$$

where $w = w(f)$ is the steering vector.

From this formula we see that any steering vector parallel to a source eigenvector will result in a sharp peak of $\hat{P}(f)$.

However, the minimum eigenvector beamformer is not recommended for the following reasons:

- In real applications the cross-correlation matrix will be estimated via a finite average. Consequently all eigenvalues and in particular the minimum eigenvalue are estimated only within finite error bounds. This uncertainty may be negligible for large eigenvalues but plays an important role for the minimum eigenvalue. As the minimum eigenvalue is relatively uncertain, the corresponding eigenvector is nearly unpredictable.
- In all cases where the number of sources K is significantly less than the number of hydrophones M , or more precisely, if $K < M - 1$, then not only the signal eigenvectors but also $M - 1 - K$ noise eigenvectors will be orthogonal to the minimum eigenvector. This means that not only possible source directions may peak but also the residual "noise directions".

To overcome these problems one must first estimate the number of noise eigenvalues; secondly, one may try to combine the different noise eigenvalues and eigenvectors in some way to produce satisfactory results. The first part, namely the estimation of the number of noise eigenvalues, is a difficult decision problem. Here, for this report, we evade the problem by assuming that the number of noise eigenvectors is known a priori. Concerning the combination of the different noise eigenvalues and eigenvectors, there are two major approaches which are outlined next.

Recently Kumaresan and Tufts [7] proposed a simple concept for an optimal orthogonal beamformer. They replaced the minimum eigenvector by an optimal linear combination of all noise eigenvectors according to the following optimization:

Model

$$d = \sum_{i=1}^{M-K} b_i v_i$$

v_i is the i -the noise eigenvector

b_i is a constant to be estimated

Optimality criterion

$$|d|^2 \rightarrow \min$$

Constraint

$$d^* c = 1, \quad c \text{ is a constant}$$

Solution

$$b_i = \frac{v_i^* c}{\sum_{i=1}^{M-K} |v_i^* c|^2}$$

A second approach combines the different power estimates of all possible noise eigenvector solutions

$$\frac{1}{\hat{P}(f)} = \sum_{i=1}^{M-K} b_i \frac{1}{\hat{P}_i}$$

where b_i is a constant to be estimated, and

$$\hat{P}_i = \frac{\lambda_i}{|v_i^* w|^2},$$

where

λ_i is the i -th noise eigenvalue,
 v_i is the corresponding eigenvector, and
 $w = w(f)$ is the steering vector.

Parameter b_i has two known implementations:

$$b_i = \begin{cases} 1, & \text{Johnson and DeGraaf [8];} \\ \lambda_i, & \text{MUSIC of Schmidt [9].} \end{cases}$$

3 THEORETICAL RESULTS

3.1 Summary of the beamforming techniques

Before the analysis of the different beamformers is presented a summary of the "pseudo" power estimates is given. The expressions correspond also to the formulas programmed into the computer.

a) Notation

Correlation Matrix

$$S = \frac{1}{2T} \sum_{t=1}^T (y_t y_t^* + \tilde{y}_t \tilde{y}_t^*), \quad \tilde{y} = (y_M, \dots, y_1)^*$$

\tilde{S} is the spatial averaged correlation matrix.

Correlation Function

$$\hat{r}_k = (M - |k|)^{-1} \text{Tr}(S \Omega^k)$$

Eigenvector Equation

$$S v_i = \lambda_i v_i$$

where

λ_i is the i -th eigenvalue of S

v_i is the eigenvector to λ_i

Steering vector

$$w_k(f) = e^{-2\pi i k f}, \quad f = \frac{d}{\lambda} \cos(\omega)$$

where

d is the array spacing,

λ is the signal wave length,

ω is the steering angle.

b) Conventional Beamforming

$$\hat{P}(f) = 2\text{Re}(\hat{r} w(f))/M, \quad \hat{r}_0 = r_0/2$$

Blackman-Tukey

$$\hat{r}_k = r_k \rho(|k| < M)$$

Wiener

$$\hat{r}_k = r_k \left(1 - \frac{|k|}{M}\right) \rho(|k| < M)$$

c) Adaptive Beamforming

$$\hat{P}(f) = \frac{1}{w^* S^{-1} w}$$

d) Maximum Entropy Beamforming

$$\hat{P}(f) = \left| \frac{c^T \tilde{S}^{-1} c}{c^T \tilde{S}^{-1} w} \right|^2$$

e) Orthogonal Beamforming

Optimal Eigenvector Method

$$\hat{P}(f) = \left| \frac{c^T \left(\sum_{i=1}^{M-K} v_i v_i^* \right) c}{c^T \left(\sum_{i=1}^{M-K} v_i v_i^* \right) w} \right|^2$$

Harmonic Averaging Technique

$$\hat{P}(f) = \frac{1}{w^* \sum_{i=1}^{M-K} \frac{b_i}{\lambda_i} v_i v_i^* w}, \quad b_i = \begin{cases} 1/M, & \text{Johnson} \\ \lambda_i, & \text{MUSIC of Schmidt} \end{cases}$$

3.2 Assumptions

The results presented in this chapter are based on the exact knowledge of the cross correlation function:

$$r_k = \sigma_n^2 \rho(k=0) + \sum_{i=1}^K \sigma_i^2 S_i$$

where

- σ_n^2 is the noise spectral power;
- σ_i^2 is the signal spectral power;
- S_i is the signal bearing vector;
- K is the number of signals.

The beamformer outputs, derived by using the different techniques, are presented in Figures 2 to 8. The results are based on the following parameter values:

Number of hydrophones:	$M = 32$
Order of linear predictor:	$p = 24$
Number of signals:	$K = 2$
Noise power:	$\sigma_n^2 = 0$ dB
Signal to noise ratios:	$\sigma_1^2/\sigma_n^2 = 0$ dB
	$\sigma_2^2/\sigma_n^2 = -10$ dB
Signal bearings:	$S_1 = 75/128 = 65.56^\circ$
	$S_2 = 80/128 = 77.36^\circ$

3.3 Conventional Beamforming

Outputs for the conventional beamformer are presented in Figures 2 and 3. The Blackman-Tukey method as shown in Fig. 2 is characterized by an oscillating power spectrum and relatively high sidelobe levels that tend to disguise the second source (which has a signal-to-noise ratio of -10 dB). The Wiener approach shows positive power estimates as well as lower sidelobe levels. Therefore the second, weaker source is clearly visible. However, the mainlobes are enlarged compared to those of the Blackman-Tukey method.

3.4 Adaptive Beamforming

Figure 4 presents a typical output of the Capon beamformer. The two sources can be seen very clearly. No significant sidelobes are present in the figure. The signal-to-noise ratio in source direction corresponds to the value measured with the conventional Wiener beamformer. As a consequence the Capon beamformer may be used as a power estimator.

3.5 Maximum Entropy Beamforming

Figure 5 gives the output of the Maximum Entropy Method. Two interesting features may be observed; first, the output signal-to-noise ratio is apparently twice those of the previously presented methods. Second, there are sidelobes in the form of oscillations. This is a strong indication that the extrapolation of the correlation function has not been made in an analytic way, thus verifying Lunde and Zimmer [1].

3.6 Orthogonal Beamforming

The beamformer outputs of the eigenvector techniques are given in Figures 6, 7 and 8. In these figures we see two peaks of equal level independent of the input signal-to-noise ratio.

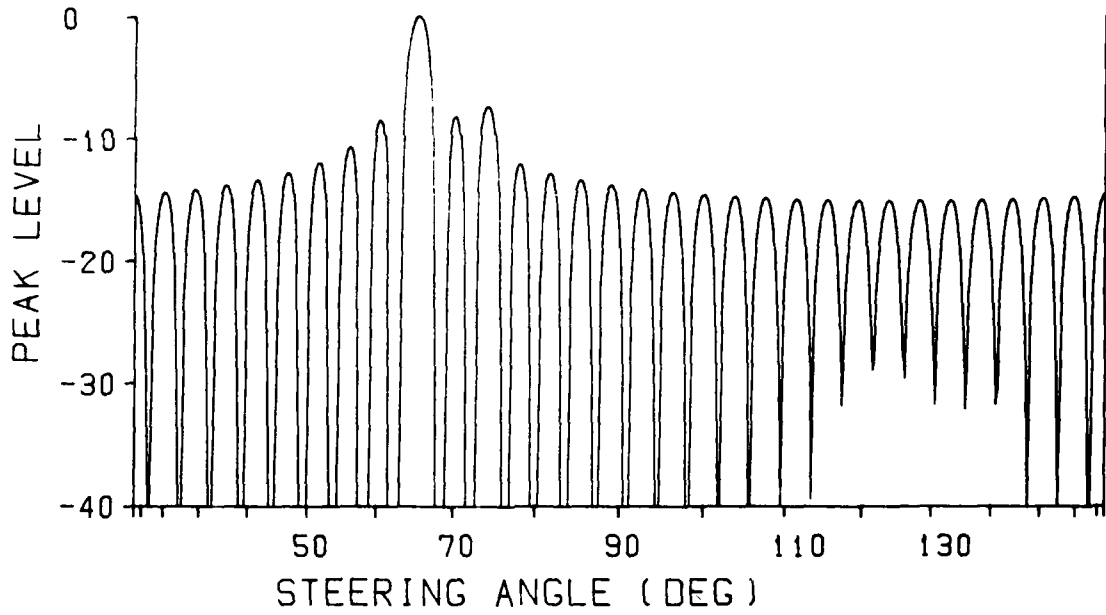


Fig. 2: Blackman-Tukey Conventional Beamforming; known correlation function.

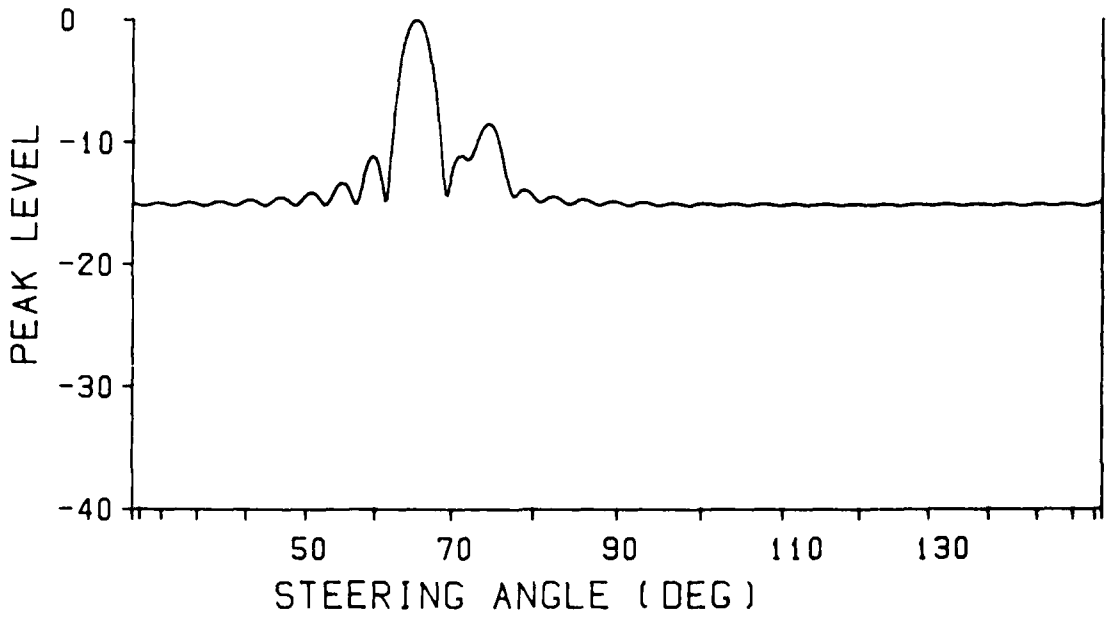


Fig. 3: Wiener Conventional Beamforming; known correlation function.

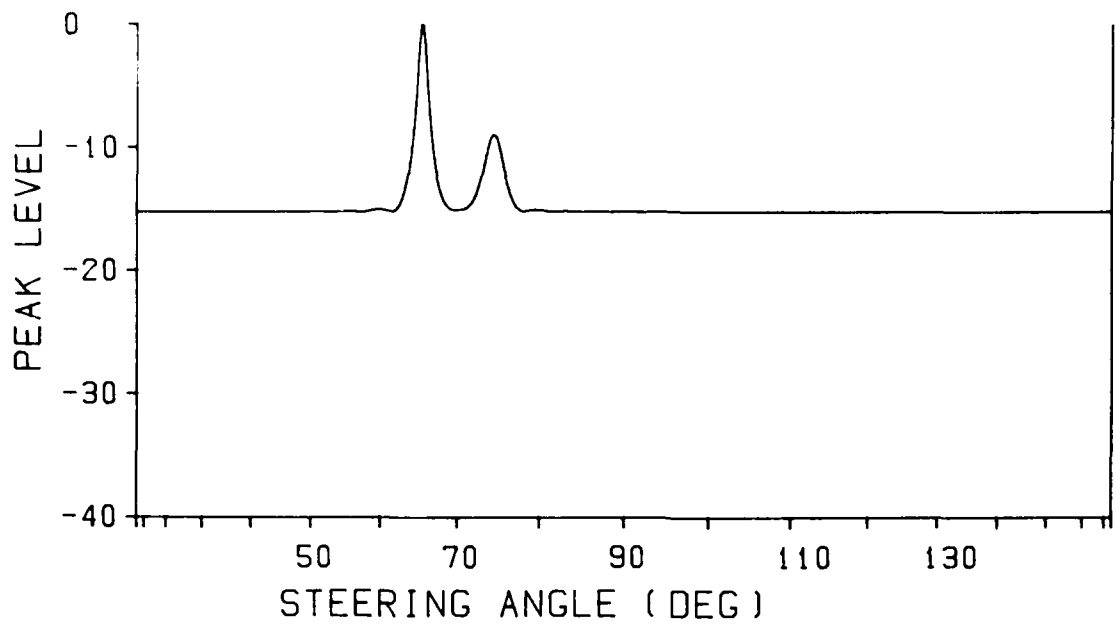


Fig. 4: Capon Adaptive Beamforming; known correlation function.

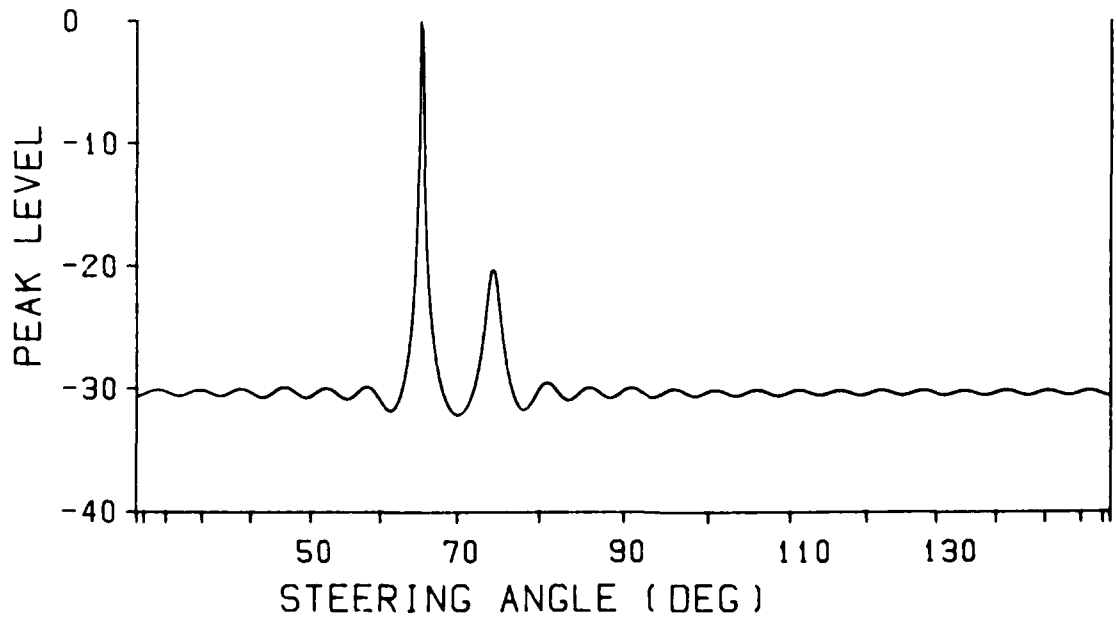


Fig. 5: Maximum Entropy Beamforming; known correlation function.

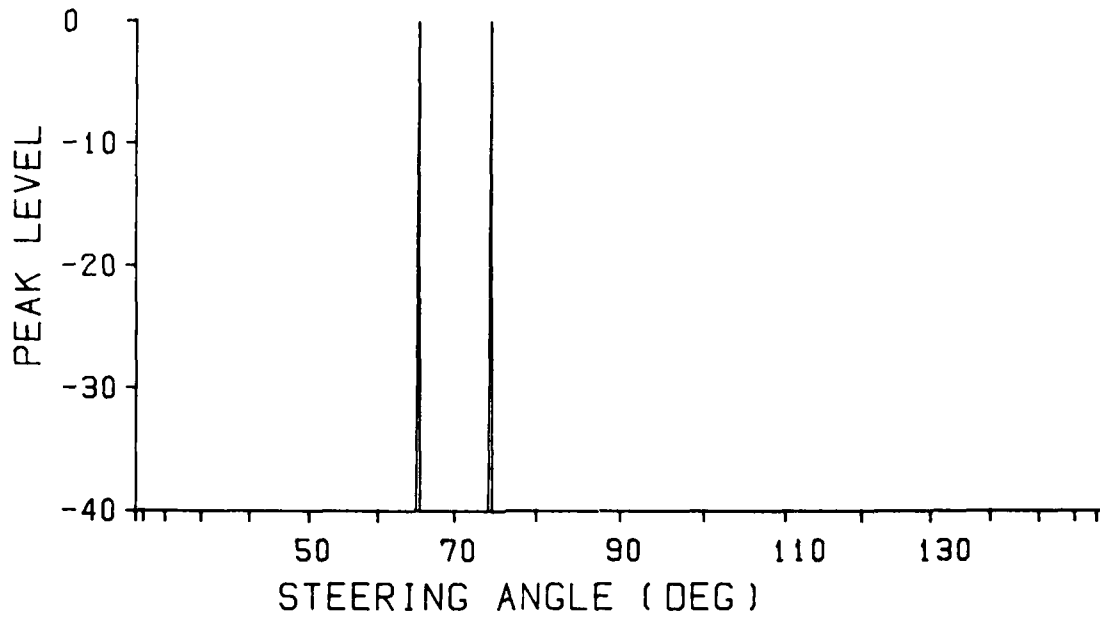


Fig. 6: Optimal Eigenvector Method; known correlation function.

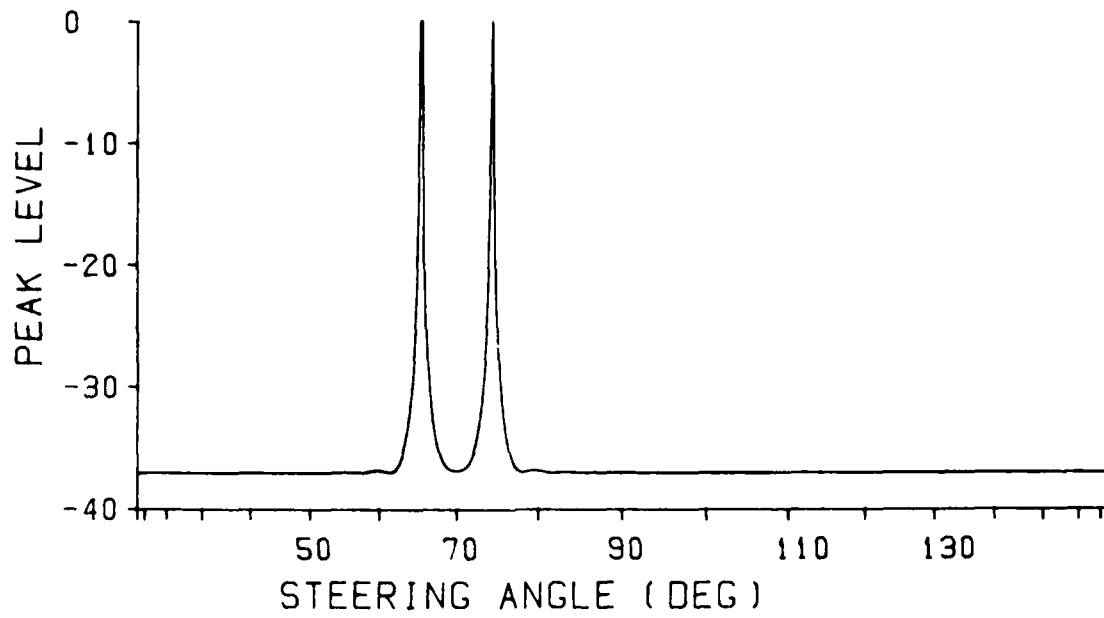


Fig. 7: Johnson Eigenvector Method; known correlation function.

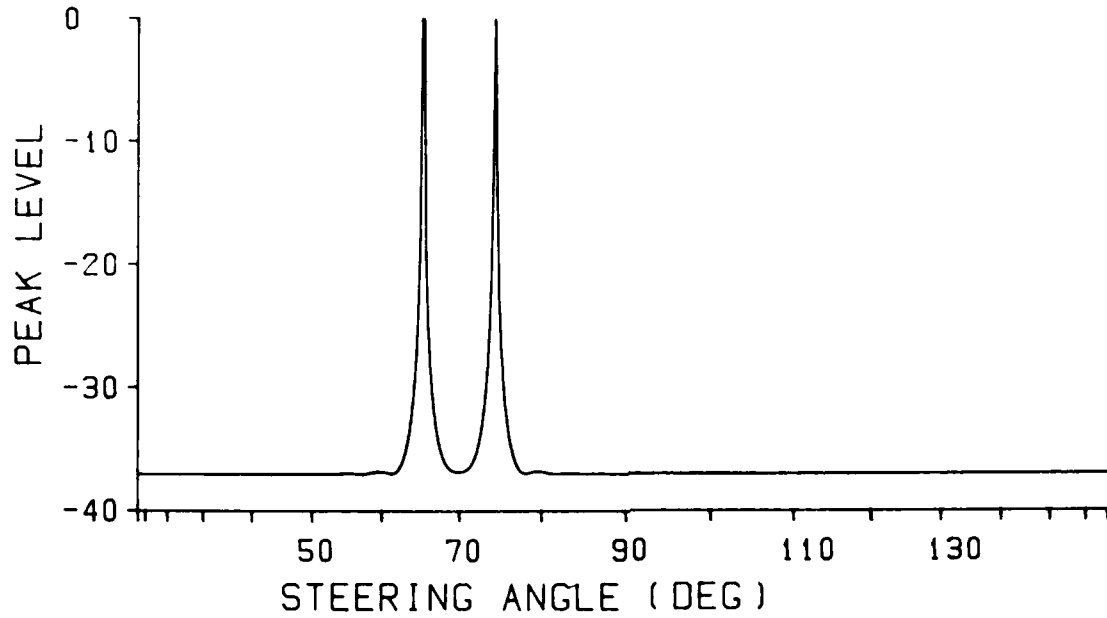


Fig. 8: Schmidt Eigenvector Method; known correlation function.

These features indicate clearly that orthogonal beamformers are direction finders and not power estimators. Further, the two techniques, which are based on harmonic averaging, show a dynamic range of about 37 dB; this range is probably due to computer limitations.

4 DETECTION PERFORMANCE

This section presents the analysis of the detection performance of the different beamforming methods described previously.

4.1 Preliminaries

A clear indication of detection performance was derived from a series of simulations. The scenario consisted of a single source of white noise. A hydrophone cross-correlation matrix was estimated by means of $NAV = 40$ averages. After beamforming, the peak level of the local maximum nearest to the direction of interest was measured (Figure 9). For each given signal-to-noise ratio this experiment was repeated 1000 times to provide sufficient data for statistical analysis. To reduce the time requirements of the simulations all seven methods were applied to the same correlation matrix.

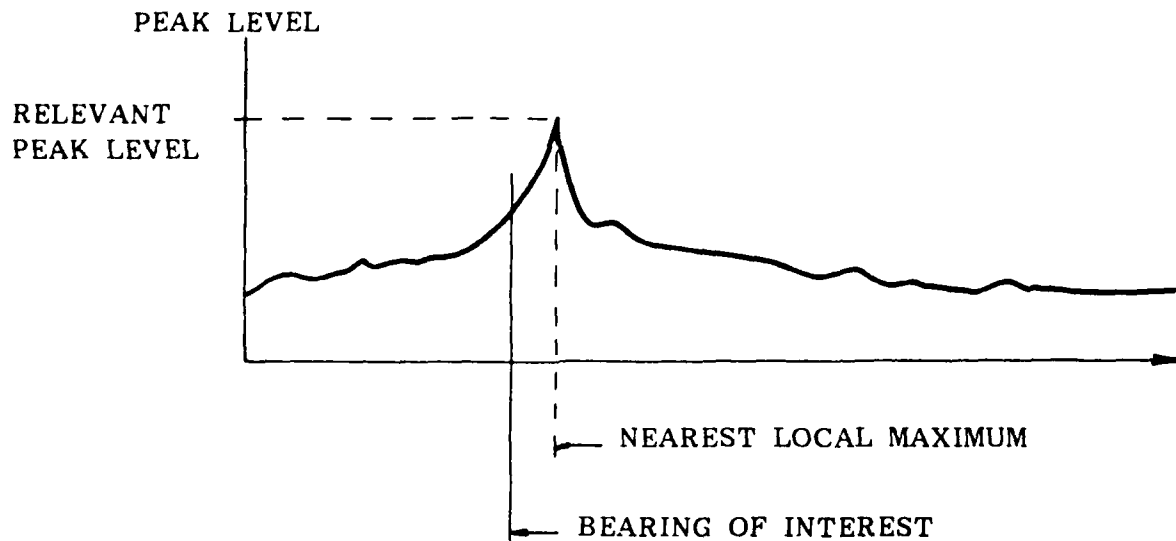


Fig.9: Definition of a local maximum.

The peak level is easily found when the signal is present. There are three possibilities for defining the distribution of noise-alone level:

Fixed beam noise distribution: distribution of the noise level in the direction of interest.

Local noise distribution: distribution of the peak level of the local maximum nearest to the direction of interest.

- Global noise distribution: distribution of the peak level of the global maximum.

Of these possibilities only the local noise distribution is consistent with the assumption that the source direction is determined by estimating the local maximum nearest to the direction of interest. Therefore this definition has been used throughout this report.

4.2 Detection probability

Appendix B provides a summary of the simulations that gave the detection performance. The cumulative probability of the peak-level estimation is plotted against its estimated level. With gaussian scaling of the probability axis (ordinate) and the peak level (abscissa) in dB, a straight line represents a log-normal distribution of the peak-level estimates.

From the cumulative distribution of the peak-level estimation we can easily deduce the detection probability (Figure 10). First we plot the noise distribution (no signal) so that the false alarm probability can be found directly from the ordinate. For every false alarm probability the abscissa gives the threshold to use to get the detection probability from the signal curves. No assumptions are made about the statistics, e.g. the peak levels of the local maxima may or may not have a normal or log-normal distribution. The selection of log-normal scaling was only made for plotting convenience.

Figure 10 provides detection probability curves for each of the seven beamforming techniques discussed in this report. The assumed false alarm probability P_{fa} was 1.35×10^{-3} . The Wiener Conventional Beamformer and Johnson Eigenvector methods provided the highest detection probabilities; the Maximum Entropy and Optimal Eigenvector methods provided the lowest.

From theoretical analysis one could assume that all eigenvector techniques are poor as detectors because they are direction finders, not power estimators. Therefore the methods of Johnson and Schmidt performed surprisingly well, probably because the theory of orthogonal beamformers assumes that the signal-bearing vectors are parallel to the signal eigenvectors and orthogonal to the noise eigenvectors. This theory requires the cross-correlation matrix to be estimated by an infinite average; this is not done in reality. As a consequence the orthogonality between signal-bearing vectors and noise-eigenvectors breaks down. Apparently the harmonic averaging of the Johnson and Schmidt techniques uses this effect to generate and stabilize an angle between the signal-bearing vector and the noise subspace that depends on the input signal-to-noise ratio of the sound source. The Optimal Eigenvector technique cannot show such a feature because of its linear averaging.

4.3 Accuracy of bearing estimation

Figure 11 is a plot of the Standard Deviation of the bearing estimation as a function of input signal-to-noise ratio for all seven techniques. The Standard Deviation has been estimated by the relation:

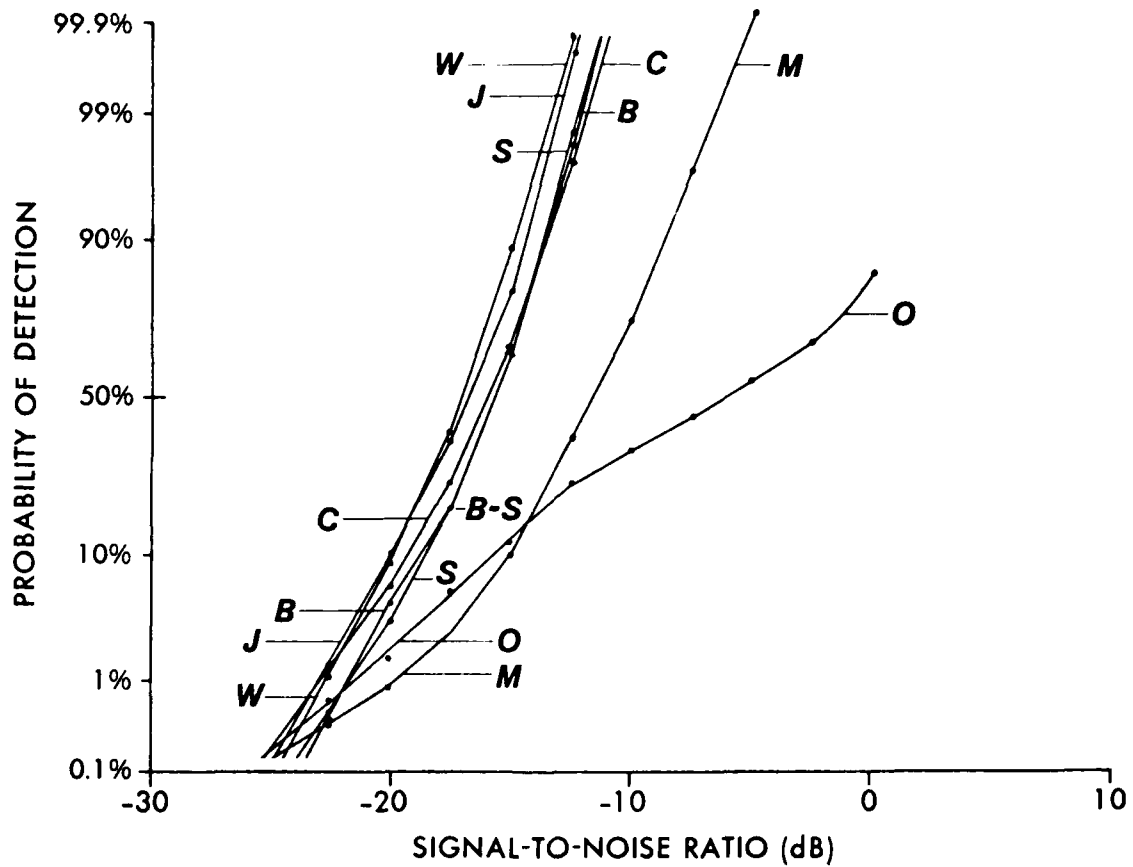


Fig. 10: Probability of detection as a function of input signal-to-noise ratio.

W: Wiener Conventional Beamformer; B: Blackman-Tukey Conventional Beamformer; C: Capon Adaptive Beamformer; M: Maximum Entropy Method(Forward- Backward Linear Predictor); O: Optimal Eigenvector Method; J: Johnson Eigenvector Method; S: Schmidt Eigenvector Method

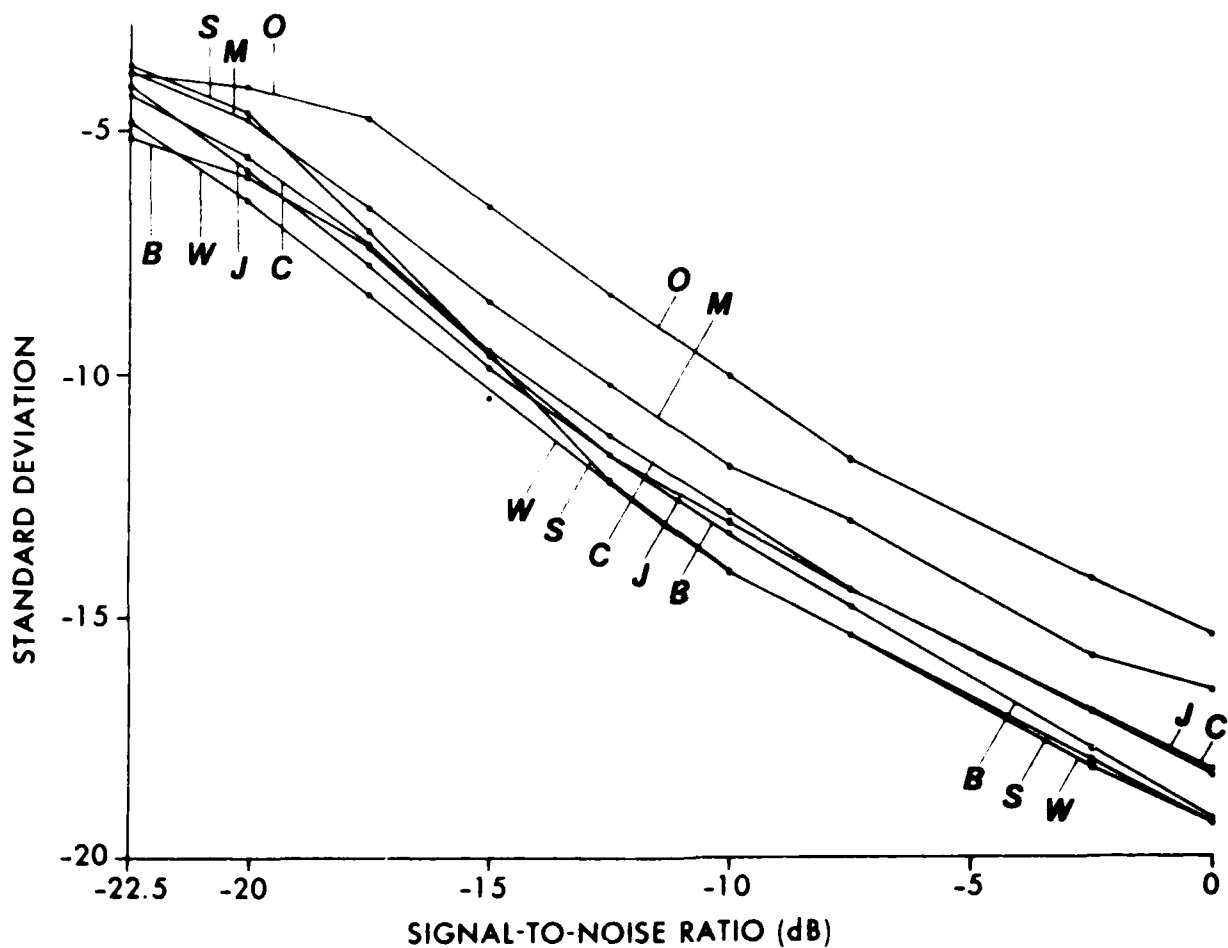


Fig. 11: Standard deviation of bearing estimation as a function of input signal-to-noise ratio.

W: Wiener Conventional Beamformer; B: Blackman-Tukey Conventional Beamformer; C: Capon Adaptive Beamformer; M: Maximum Entropy Method (Forward- Backward Linear Predictor); O: Optimal Eigenvector Method, J: Johnson Eigenvector Method; S: Schmidt Eigenvector Method

$$\sigma = \frac{\Phi_R^{-1}(1) - \Phi_R^{-1}(1/2)}{2}$$

where $\Phi_R(x)$ is the cumulative distribution of the bearing estimation.

This formula assumes a gaussian distribution for the bearing estimates. This is a good approximation for signal-to-noise ratios that are not too low. The actual values of the standard deviation have been normalized with respect to the reciprocal aperture and are plotted in log scale

The results indicate that the Wiener technique with the lowest standard deviation of all seven techniques, performs best. The Optimal Eigenvector and the Maximum Entropy techniques have the worst performance (as they did for the detection probability).

At first glance it seems surprising that the high-resolution methods perform so badly. But a closer look at these methods provides a simple explanation related to the fact that the high-resolution methods extrapolate the correlation function beyond the array aperture. The sharper the peak of a power spectrum the longer the correlation function must be. If the correlation function is not known exactly within the array aperture, then the extrapolation may be unstable and in most cases will amplify the influence of the noise on the estimation performance.

5 RESOLUTION PERFORMANCE

5.1 Scenario

To study the resolution capabilities of the different beamformers the following simulations were repeated 1000 times: two closely spaced point sources in white noise are assumed to have equal signal-to-noise ratio of 0 dB and given varying separations. The directions of interest are given by the simulated source directions. The datum is ignored if a single local maximum is nearest to both directions of interest and therefore no resolution is observed. The sources are considered as being resolved when there are two local maxima.

Three quantities are of interest:

- the bias of the bearing estimation,
- the deviation of the bearing estimation,
- the probability of resolution.

5.2 Resolution probability

Appendix B presents the statistics of the two source-bearing estimation experiments. The probability axis (ordinate) is again scaled such that a normal distribution results in a straight line. The abscissa measures the separation in units of $1/\text{aperture}$. The nominal source separation at which the simulation has been carried out is the curve parameter.

Figure 12 presents the main results of the resolution experiments. Here the probability that two sources are resolved is plotted against the separation of these two sources. The probability is given in gaussian scaling and the source separation is measured in beam number units (of $1/\text{aperture}$).

As expected, the Wiener conventional beamformer performed poorest. On the other hand the high-resolution techniques were able to resolve the two sources even when they had a small separation.

Except for the Optimal Eigenvector technique, all the high-resolution methods have a rather similar performance. We can therefore deduce that at least for simulated data the effective beamformer aperture of these high-resolution techniques is of the same order of magnitude for all of them.

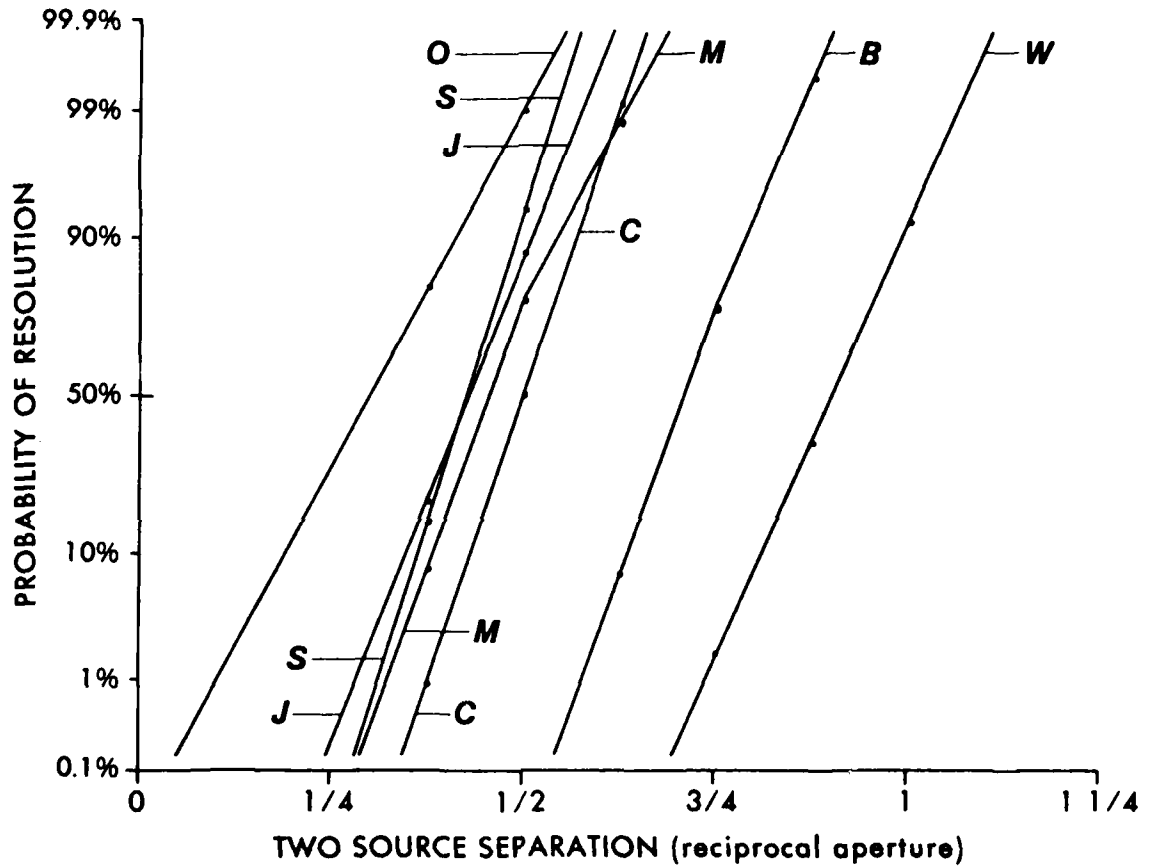


Fig. 12: Probability of resolution as a function of two source separation (measured in units of 1/aperture)

W: Wiener Conventional Beamformer; B: Blackman-Tukey Conventional Beamformer; C: Capon Adaptive Beamformer; M: Maximum Entropy Method (Forward- Backward Linear Predictor); O: Optimal Eigenvector Method; J: Johnson Eigenvector Method; S: Schmidt Eigenvector Method

6 SUMMARY

This report presents a statistical analysis of seven high-resolution beamforming techniques. A comparison has been made between the conventional techniques on the one hand (Wiener, B-T) and conceptually different high-resolution methods on the other hand. These high-resolution techniques have been selected from three groups: Adaptive (Capon), Maximum Entropy (Max-Ent) and Orthogonal (Opt-Eig., Johnson, Schmidt) Beamformers.

Table 1 compares the statistical performance of the seven techniques with respect to detection, accuracy and resolution.

TABLE 1
Performance Statistics

Method	Detection	Accuracy	Resolution
Wiener	1.0	1.0	1.0
B-T	0.9	0.8	1.3
Capon	0.9	0.7	1.8
Max-Ent	0.7	0.6	2.0
Opt-Eig	0.4	0.4	3.0
Johnson	1.0	0.8	2.1
Schmidt	0.9	1.0	2.1

This table is based on the following assumptions:

- the detection and resolution performance measures can be taken as corresponding to the 50% point in the probability curves. The detection performance is measured in dB and the resolution performance is measured in multiple apertures.
- the accuracy measure can be represented by the standard deviation at an input signal-to-noise ratio of -10 dB (equivalent to a conventional output signal-to-noise ratio of 5 dB).
- the actual values can be related to the conventional Wiener beamformer to yield a quantitative comparison of the different techniques.

From Table 1 we can conclude that improved resolution performance of the high-resolution methods is gained at the cost of a more or less significant decrease in accuracy and detection performance. In particular the high-resolution Maximum Entropy and Optimal Eigenvector techniques show this behaviour clearly. These techniques may be understood as vector techniques in which the power estimate is based on the computation of a single

vector. The other high-resolution techniques (Capon, Johnson, Schmidt) may be called matrix techniques because they use the hydrophone cross-correlation matrix (or a part of it) to get the power estimate. These three matrix techniques show a detection performance only slightly decreased with respect to the reference technique (Wiener). This is surprising, at least for the orthogonal beamformers of Johnson and Schmidt; these two methods are designed to be direction finders, not power estimators. For perfectly known cross-correlation matrices they would indicate the source direction with infinitely large spikes. However, we have only a non-perfect estimate of the correlation matrix, yielding statistical fluctuations of the peaks of the estimator. Therefore a paradox arises, namely that the poor statistics based on finite averaging of the cross-correlation matrix enable us to use the orthogonal beamformers as detectors.

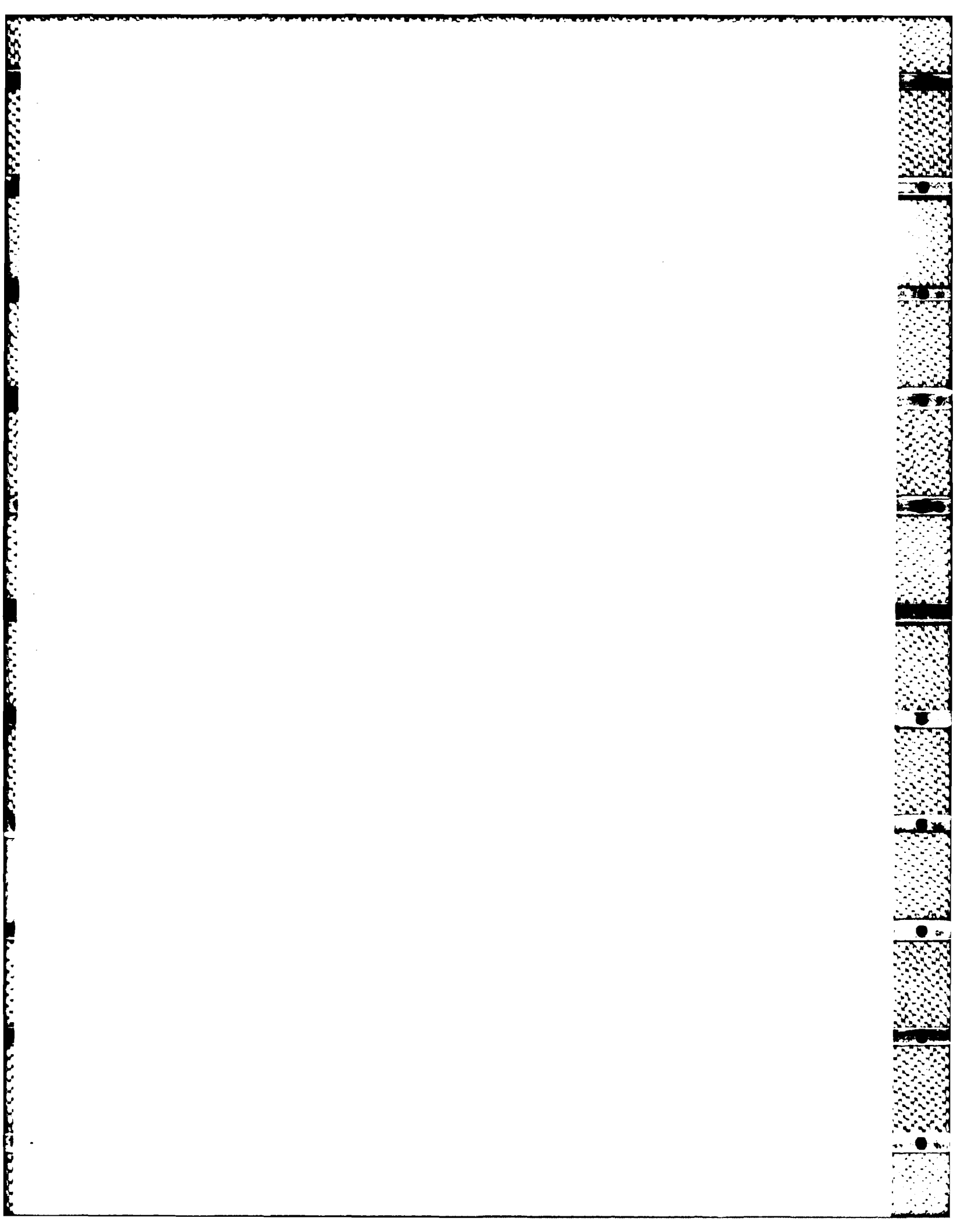
Another important conclusion from Table 1 relates to the accuracy values. None of the techniques is more accurate than the conventional Wiener technique. The consequence is clear: sharp peaks in the beamformer output do not indicate more accurate bearing estimations; they are only necessary to achieve higher resolutions. Again the two vector methods (Max-Ent; Opt-Eig) show the worst performance while the difference between the matrix-based orthogonal beamformers (Johnson, Schmidt) is less significant.

Concerning the resolution performance the three matrix techniques (Capon, Johnson, Schmidt), these do not perform as well as the vector techniques. However, all high-resolution techniques show an increased effective aperture that is at least 1.8 times greater than the conventional (real) aperture.

On this basis one can say that the high-resolution methods showed increased resolution performance; however, in cases where there is no resolution problem they did not provide more accurate bearing estimates than the conventional methods. Because any increased resolution is based on the extrapolation of the hydrophone cross-correlation function, the influence of the noise on such an extrapolation must be controlled very carefully.

REFERENCES

1. LUNDE, E.B. and ZIMMER, W.M.X. Passive sonar data processing, propagation models and the data cross correlation matrix: a survey. SACLANTCEN SR-84. La Spezia, Italy, SACLANT ASW Research Centre, 1985. [AD A 156 812]
2. NUTTALL, A.H. Spectral analysis of a univariate process with bad data points, via maximum entropy and linear predictive techniques, NUSC TR5303. New London, CT, Naval Underwater Systems Center, 1976.
3. CAPON, J., et al Multidimensional maximum likelihood processing of a large aperture seismic array *Proceedings of the IEEE*, 55, 1967 : 192 -211.
4. JAYNES, E.T. On the rationale of maximum-entropy methods. *Proceedings of the IEEE*, 70, 1982: 939- 952.
5. REIF, F. Fundamentals of statistical and thermal physics. New York, NY, McGraw-Hill, 1965.
6. KAY, S.M. and MARPLE, S.L. Jr. Spectrum analysis - a modern perspective *Proceedings of the IEEE*, 69, 1981 : 1380—1419 E, 69, 1981: 1380-1419.
7. KUMARESAN, R. and TUFTS, D.W. Estimating the angles of arrival of multiple plane waves. *IEEE Transaction on Aerospace and Electronic Systems*, 19, 1983: 134—139.
8. JOHNSON, D.H. and DEGRAAF, S.R. Improving the resolution of bearing in passive sonar arrays by eigenvalue analysis. *IEEE Transactions on Acoustic, Speech and Signal Processing*, 30, 1982: 638—647.
9. SCHMIDT, R. Multiple emitter location and signal parameter estimation. In: *Proceedings, Spectral estimation workshop*. Rome, NY, Rome Air Development Center, 1979: 243—258.
10. ZIMMER, W.M.X. Multiple Beamforming. SACLANTCEN SM-181. La Spezia, Italy, SACLANT ASW Research Centre, 1985.



APPENDIX A

Further comments on the beamformer output

The definition of beamformer output as used throughout this report is not free of problems. In particular the construction of high-resolution beamformers would appear to emphasize the direction-finding behaviour rather than the power estimation performance. Suppose we drop the requirement that the high-resolution beamformer should be a power estimator. What can we do to get not only the source bearing but also the power estimates? We could take the estimated source directions and insert them into an optimal power estimation scheme such as the maximum likelihood parameter estimation technique. However, this approach only solves the problem of the decreased detection performance of the high-resolution methods. To improve the accuracy of the bearing estimation we have to select a nonlinear maximum likelihood approach which now has the bearing of the different sources as additional unknown parameters. As a consequence the computational workload will increase enormously. In this case the high-resolution direction finder would act as a preprocessor for a multivariant parameter estimation technique [10]. It is not yet clear under which conditions the trade-off between optimal performance and computational burden may favour this parameter estimation approach to high-resolution beamforming.

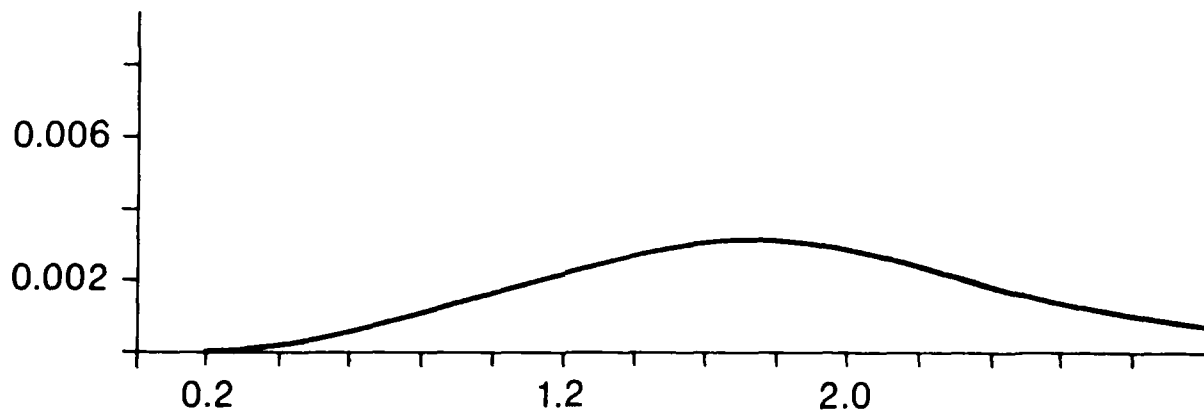
APPENDIX B

Summary of the Single-Source simulations

In this appendix the results of the single-source simulations for the seven different beam-forming techniques are summarized by plots of cumulative distributions. In all of the plots the measured peak level is plotted along the abscissa in dB and the cumulative probability is plotted along the ordinate according to a gaussian scaling. The gaussian error function has been approximated by

$$\Phi(x) = (1 + \sqrt{1 - \exp(-2x^2/\pi)})/2$$

where the plus sign is selected for $x > 0$ and the minus sign for $x < 0$. The error made by this approximation is given in the following figure.



Error due to approximation of the error function

For each plot (Figs. B1 to B7) the signal curves rise with increasing peak-level and give the probability of the peak level being less than the value at the abscissa. The noise curve on the other hand is decreasing with increasing abscissa and indicates the probability of the peak level being greater than the value of the abscissa. This value also corresponds to the false alarm probability.

Figures B4 (Maximum Entropy) and B5 (Optimum Eigenvector) are incomplete because there was insufficient data. These techniques, even on a logarithmic scale, have such a wide distribution that 1000 repetitions are not sufficient to produce adequate statistical data.

SACLANTCEN SR-104

The Johnson Eigenvector method (Fig. B6) yet again shows well-behaved, nearly log-normal distributions.

The Schmidt Eigenvector method (Fig. B7) provides an unexpected feature. The statistics strongly indicate that the distributions have a lower cut-off at 0 dB. Of 1000 peaks, none was measured below this value. The construction of this algorithm may explain this phenomenon; the true noise eigenvalues are replaced by unity (i.e., 0 dB).

The Schmidt Eigenvector, the Maximum Entropy and the Optimal Eigenvector methods show that basing the performance analysis only on first and second order statistics rather than on the complete probability distribution can be misleading.

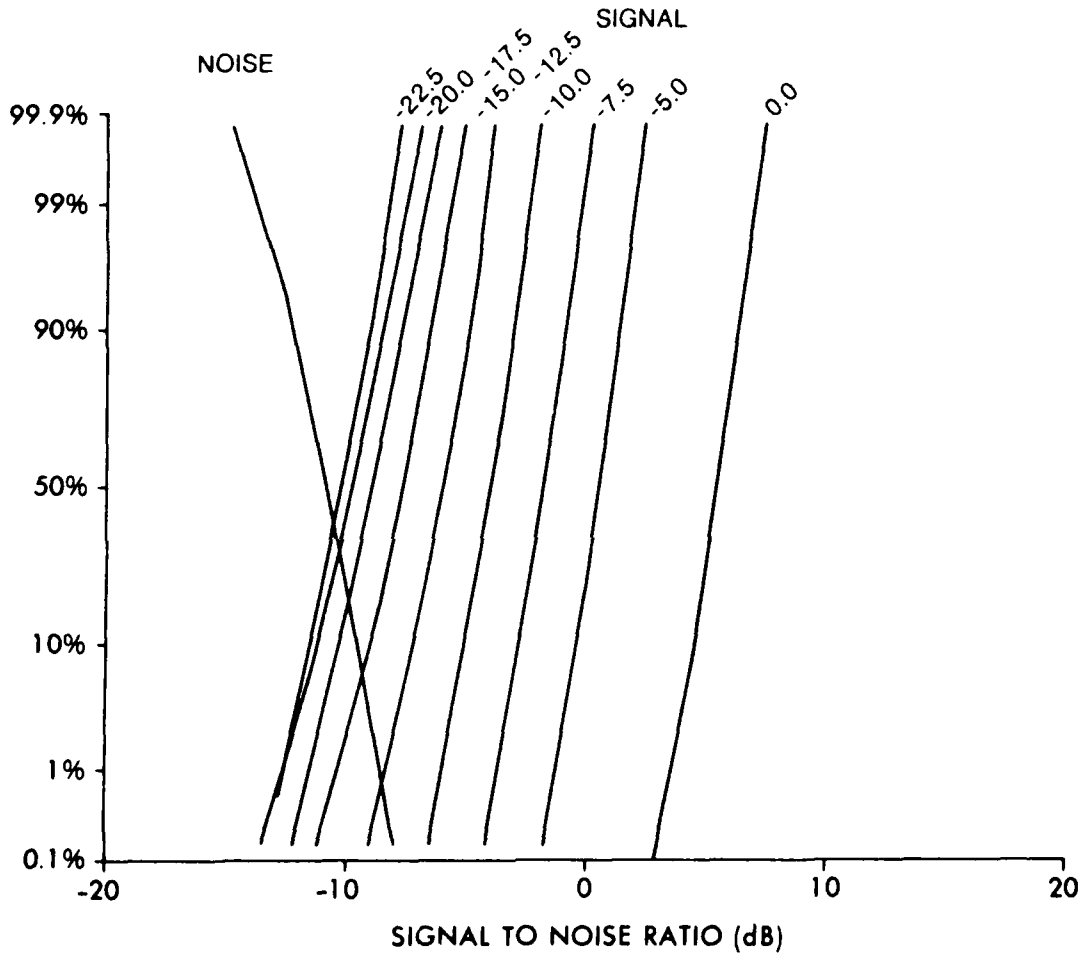


Fig. B1: Blackman-Tukey Conventional Beamformer

Probability of the peak-level of a single source. Parameter is input signal-to-noise ratio.

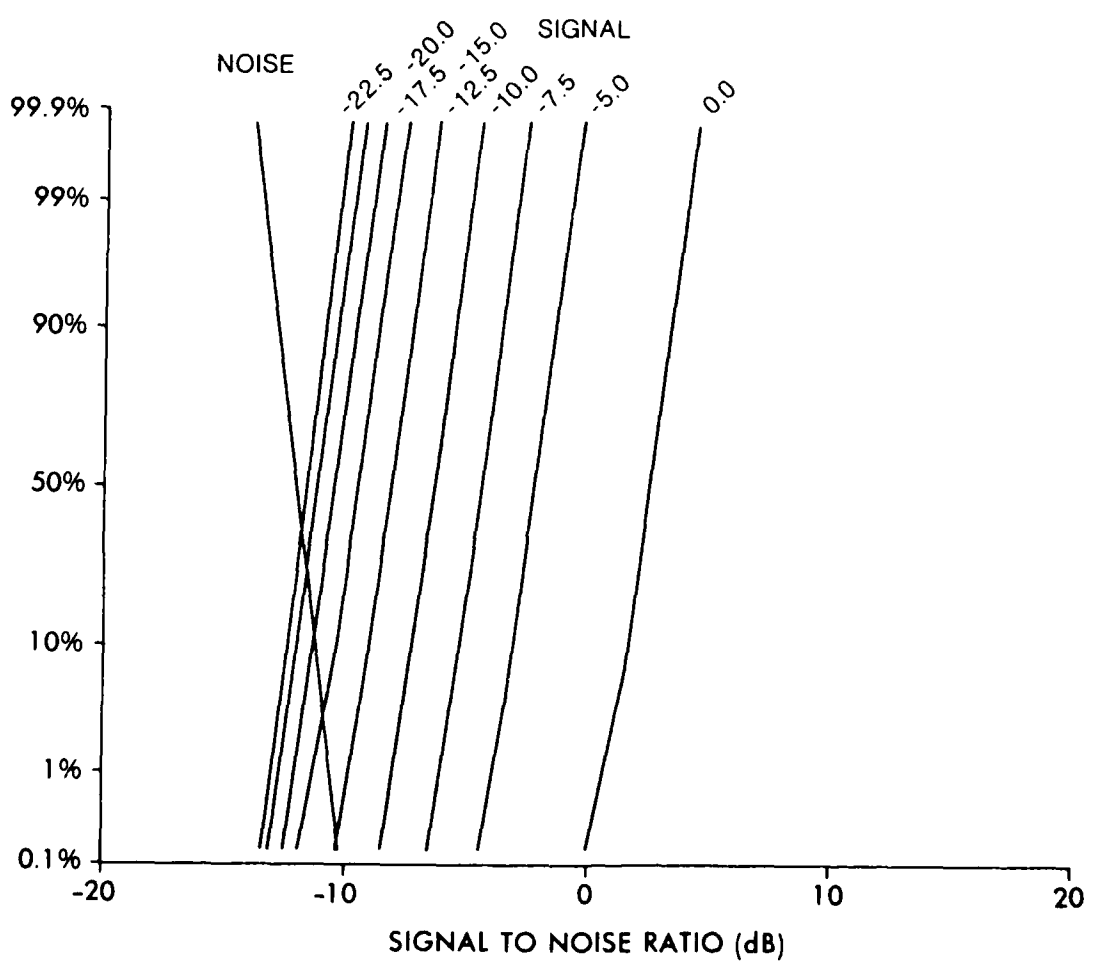


Fig. B2: Wiener Conventional Beamformer

Probability of the peak-level of a single source. Parameter is input signal-to-noise ratio.

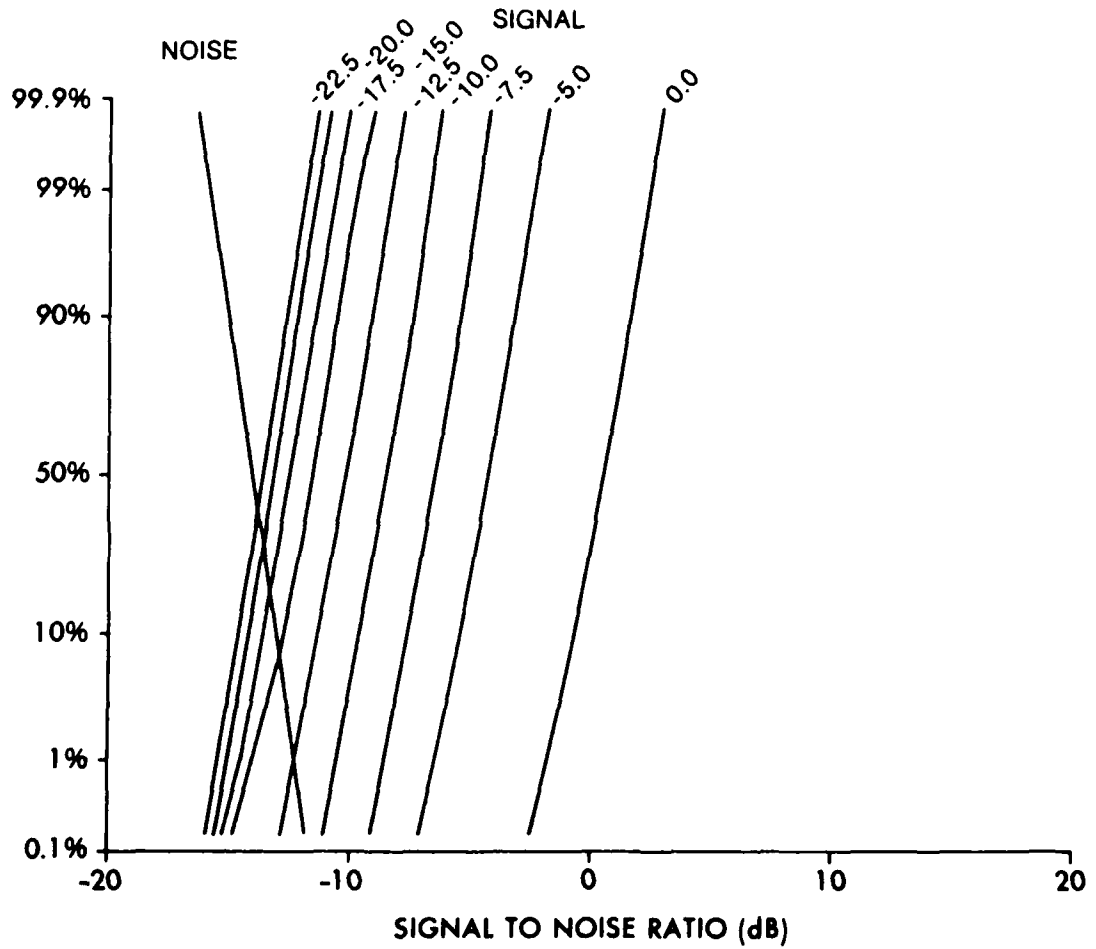


Fig. B3: Capon Adaptive Beamformer

Probability of the peak-level of a single source. Parameter is input signal-to-noise ratio.

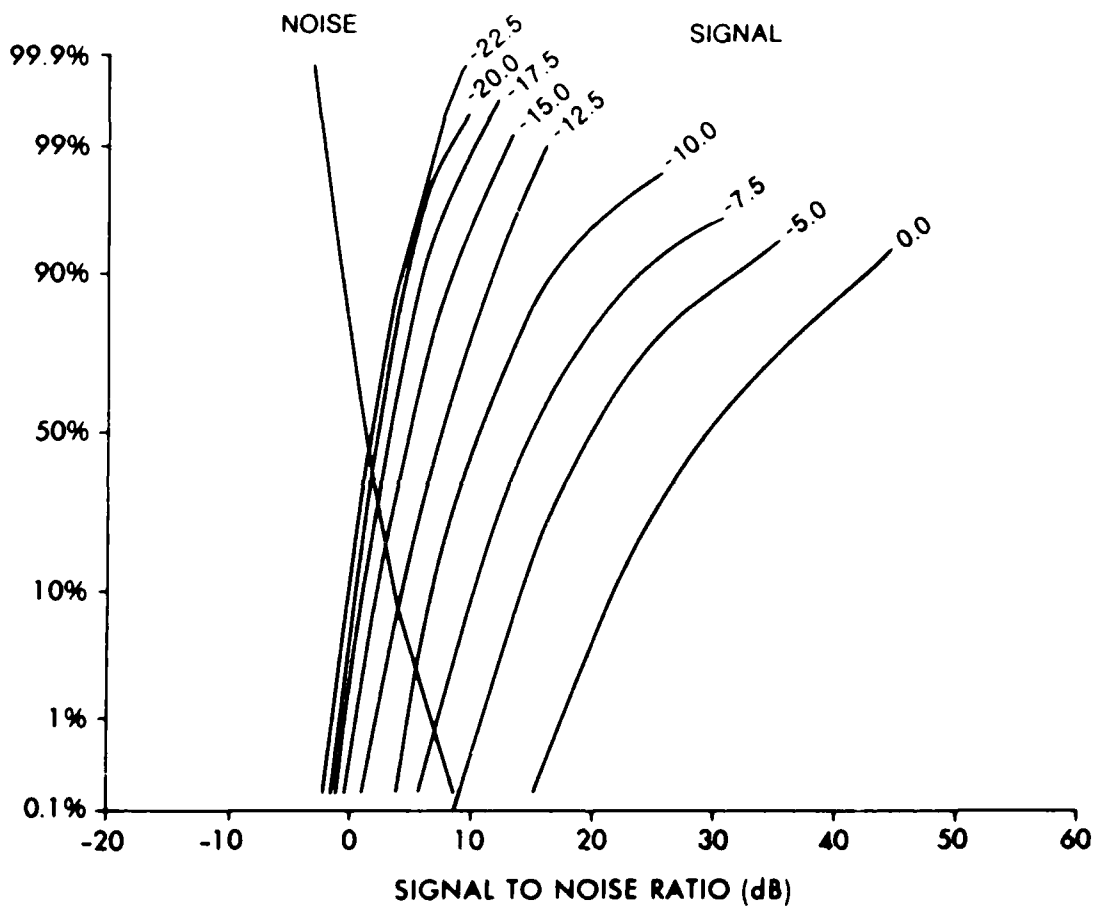


Fig. B4: Maximum Entropy Method

Probability of the peak-level of a single source. Parameter is input signal-to-noise ratio.

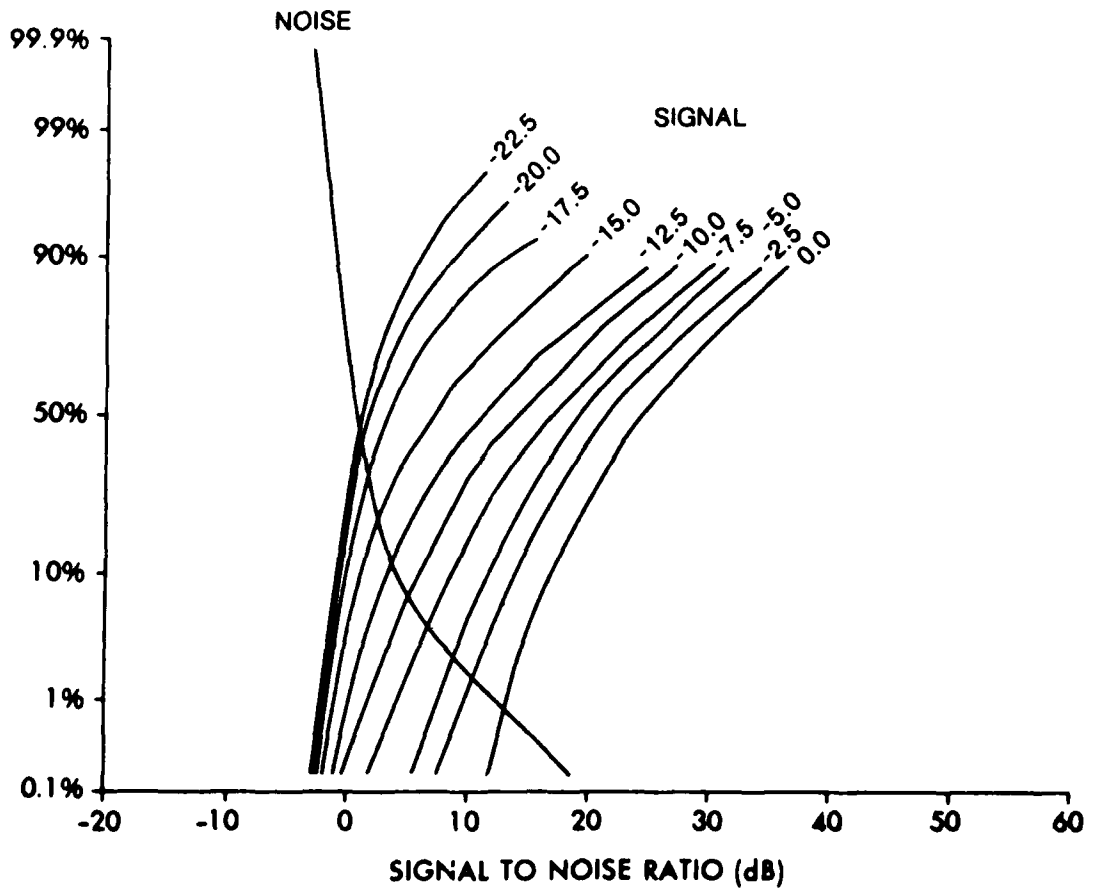


Fig. B5: Optimal Eigenvector Method

Probability of the peak-level of a single source. Parameter is input signal-to-noise ratio.

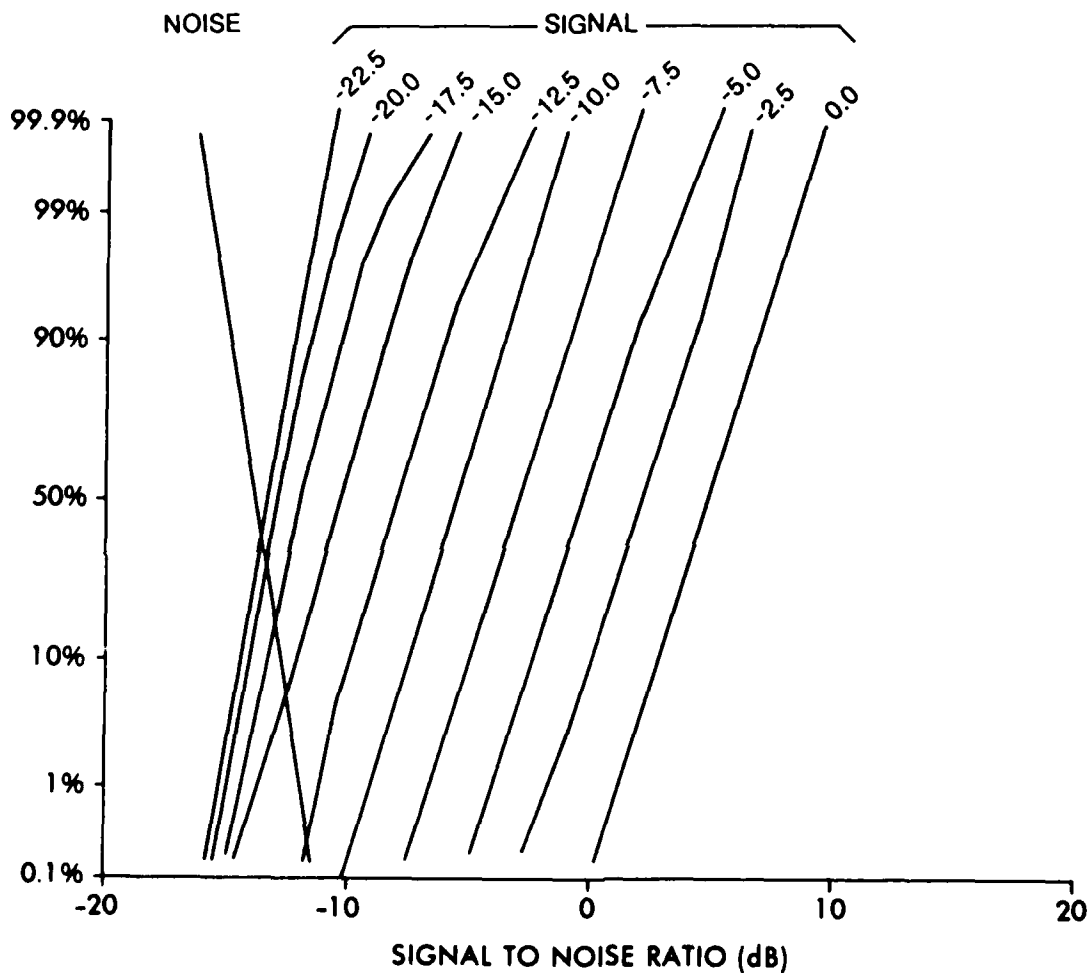


Fig. B6: Johnson Eigenvector Method

Probability of the peak-level of a single source. Parameter is input signal-to-noise ratio.

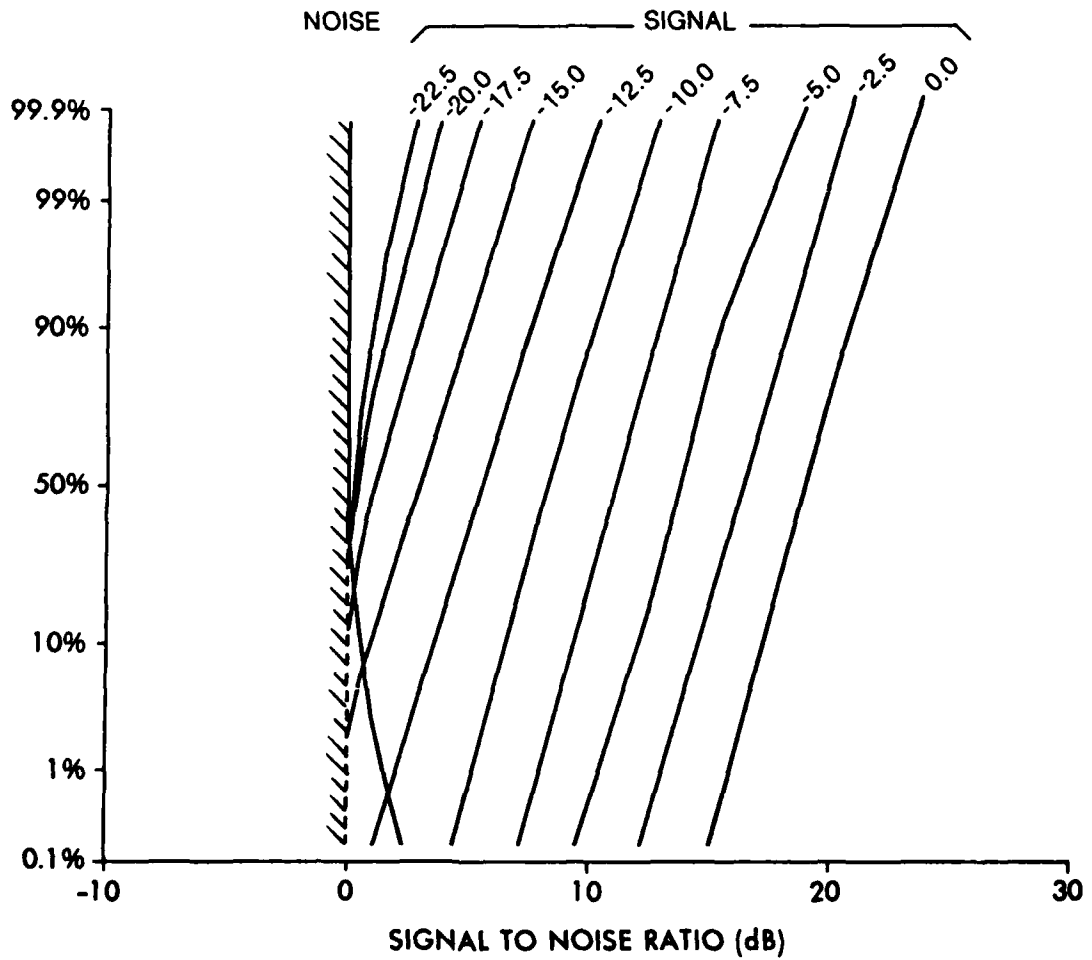


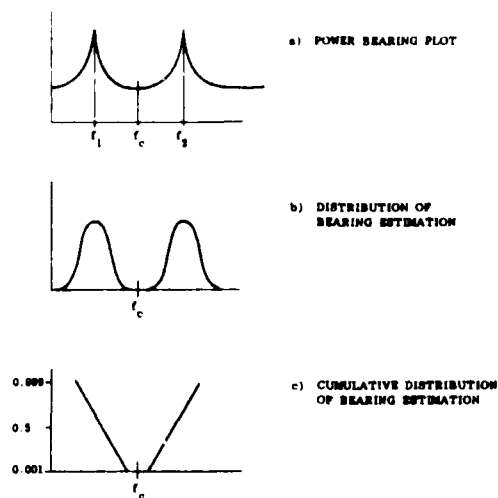
Fig. B7: Schmidt Eigenvector Method

Probability of the peak-level of a single source. Parameter is input signal-to-noise ratio.

APPENDIX C

Summary of the two-source simulations

This appendix contains the results of the two-source simulations. The approach that was used to plot the bearing estimation is illustrated in the following figure:



- a. *Every experiment in which the two sources were resolved has been used to estimate the bearings of the sources.*
- b. *The ensemble of all the successful experiments yielded the distribution of bearing estimations.*
- c. *The distributions have been plotted cumulatively so that one can read directly the probability of the individual bearing estimate being closer to the common bearing centre. Ignoring the failed experiments results in a plateau between the two cumulative distributions. The ordinate value at which the plateau is found is nothing more than the probability that the resolution experiment will fail.*

Concept of data presentation

Figures C1 to C7 present the cumulative distributions for all seven beamformers. The probability axis (ordinate) is again scaled such that normal distributions result in a straight line. The abscissa measures the separation in beam numbers (cosine scale). Again 1 unit corresponds to the reciprocal aperture and the source separation is given as parameter.

As expected, the bearing estimates are normally distributed only for wide separations. As the two sources close, the gaussian behaviour of the distribution is lost, resulting in long tails towards the common centre bearing, and the two sources start to interact. This interaction results in resolution failure when the sources are very close.

The non-gaussian behaviour at close separations shows also that simple second order statistics cannot properly describe the resolution performance. However the figures may be used to check the bias by comparing the simulated separation with the distance of the medians; the sensitivity of the bearing estimation may be found by taking the derivative of the cumulative distribution; and the resolution probability can be read directly.

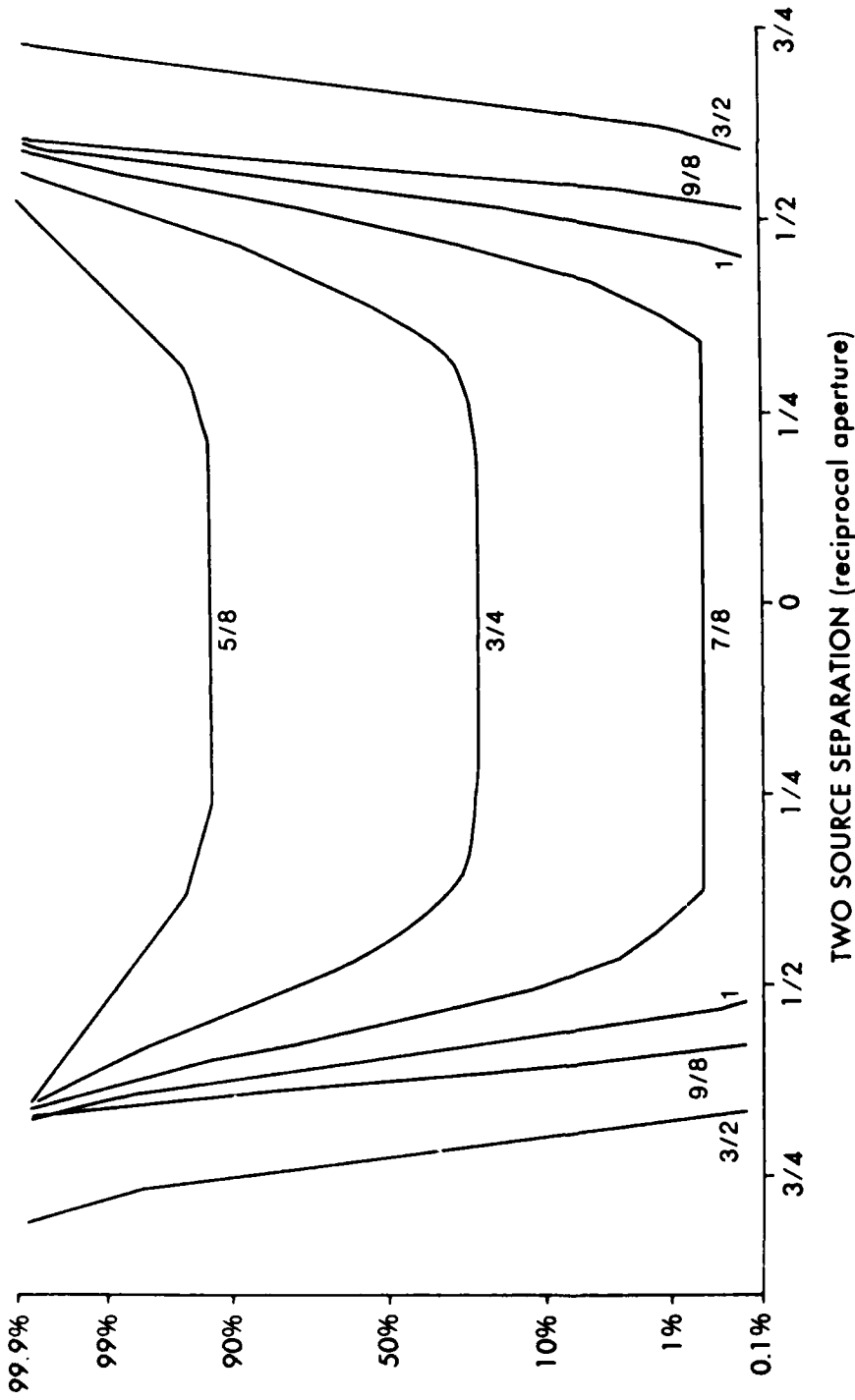


Fig. C1: Blackman-Tukey Conventional Beamformer

Probability of two source bearing estimation; the parameter is source separation measured in $1/\text{aperture}$.

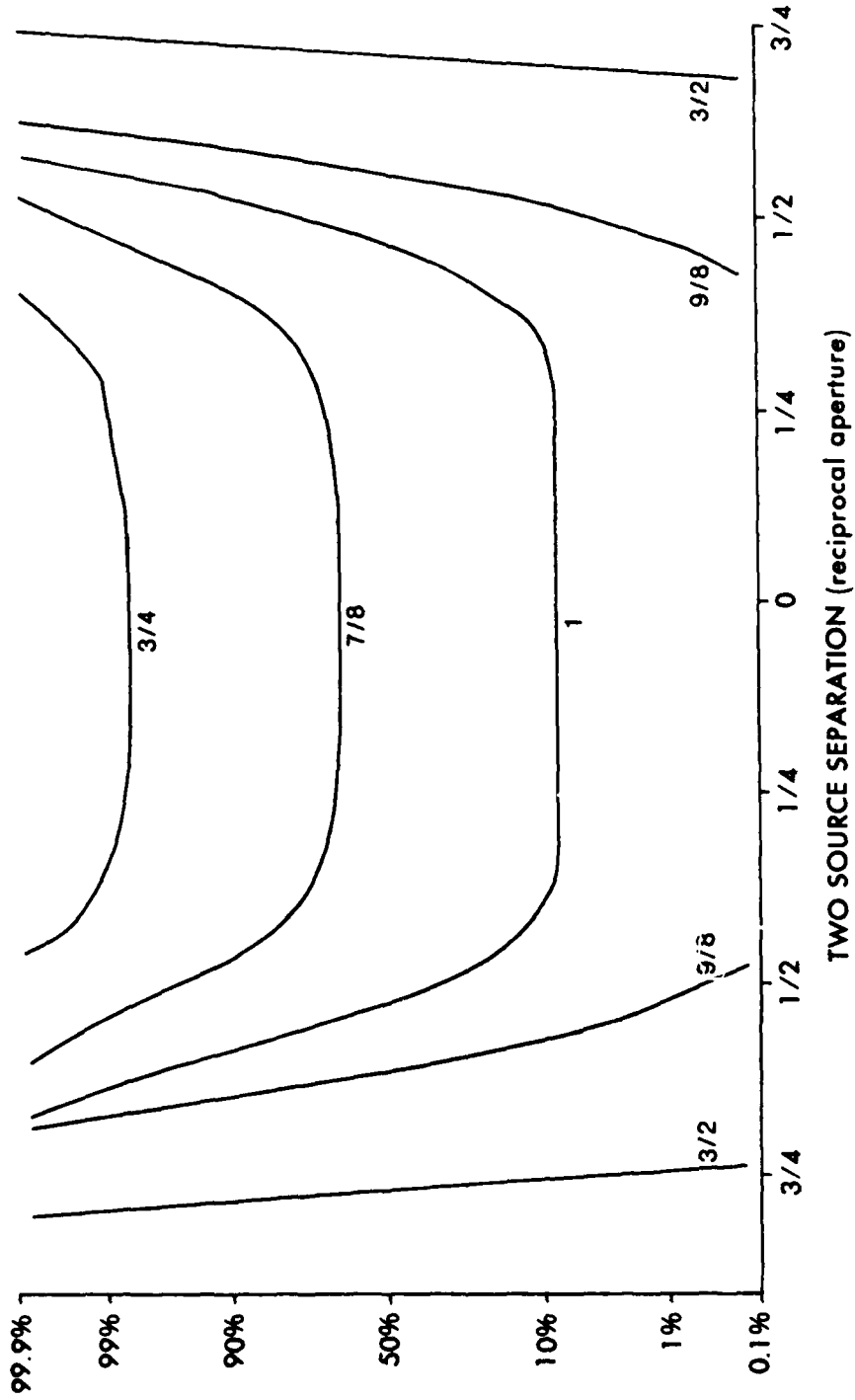


Fig. C2: Wiener Conventional Beamformer
 Probability of two source bearing estimation; the parameter is source separation measured in $1/\text{aperture}$.

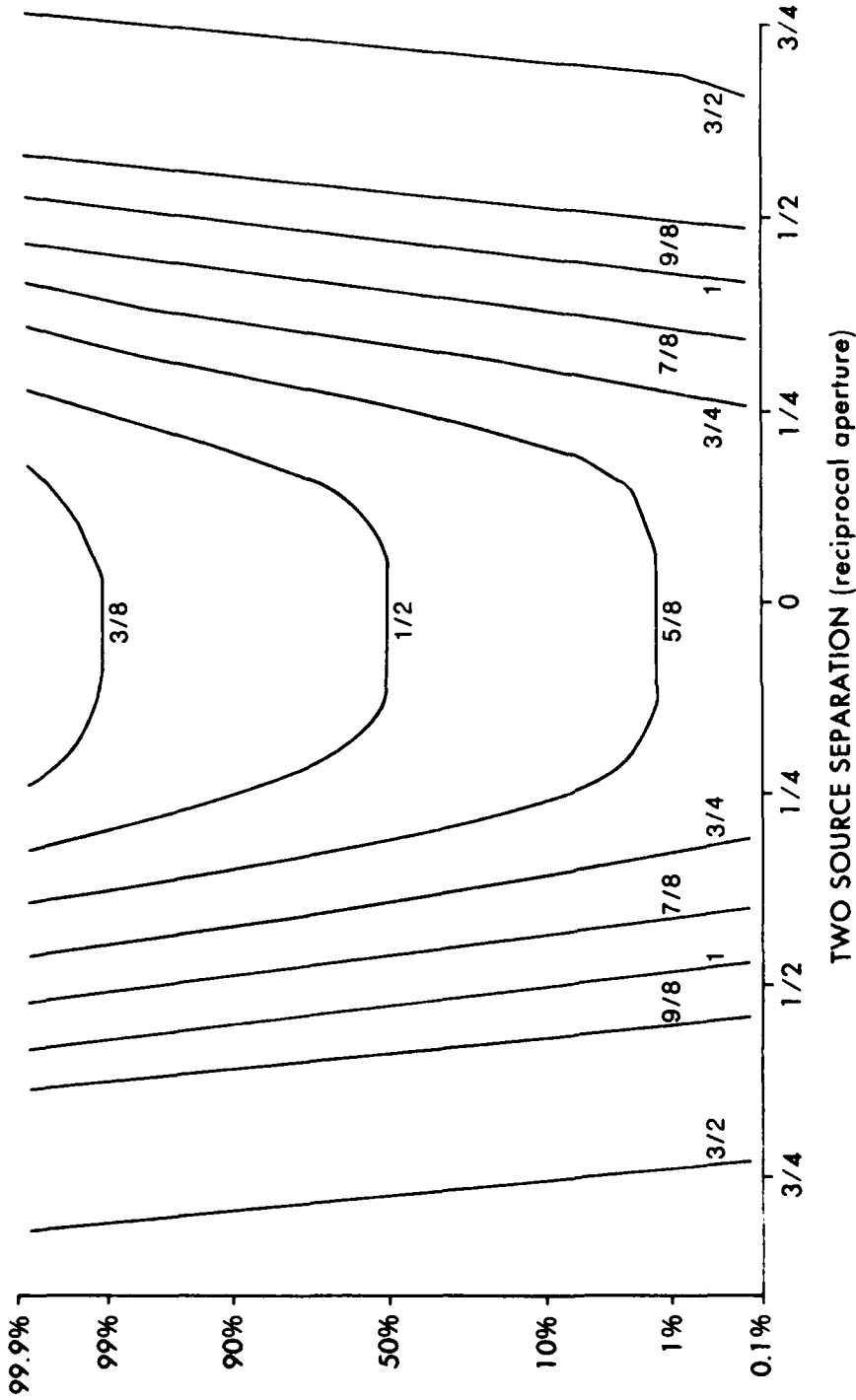


Fig. C3: Capon Adaptive Beamformer

Probability of two source bearing estimation; the parameter is source separation measured in $1/\text{aperture}$.

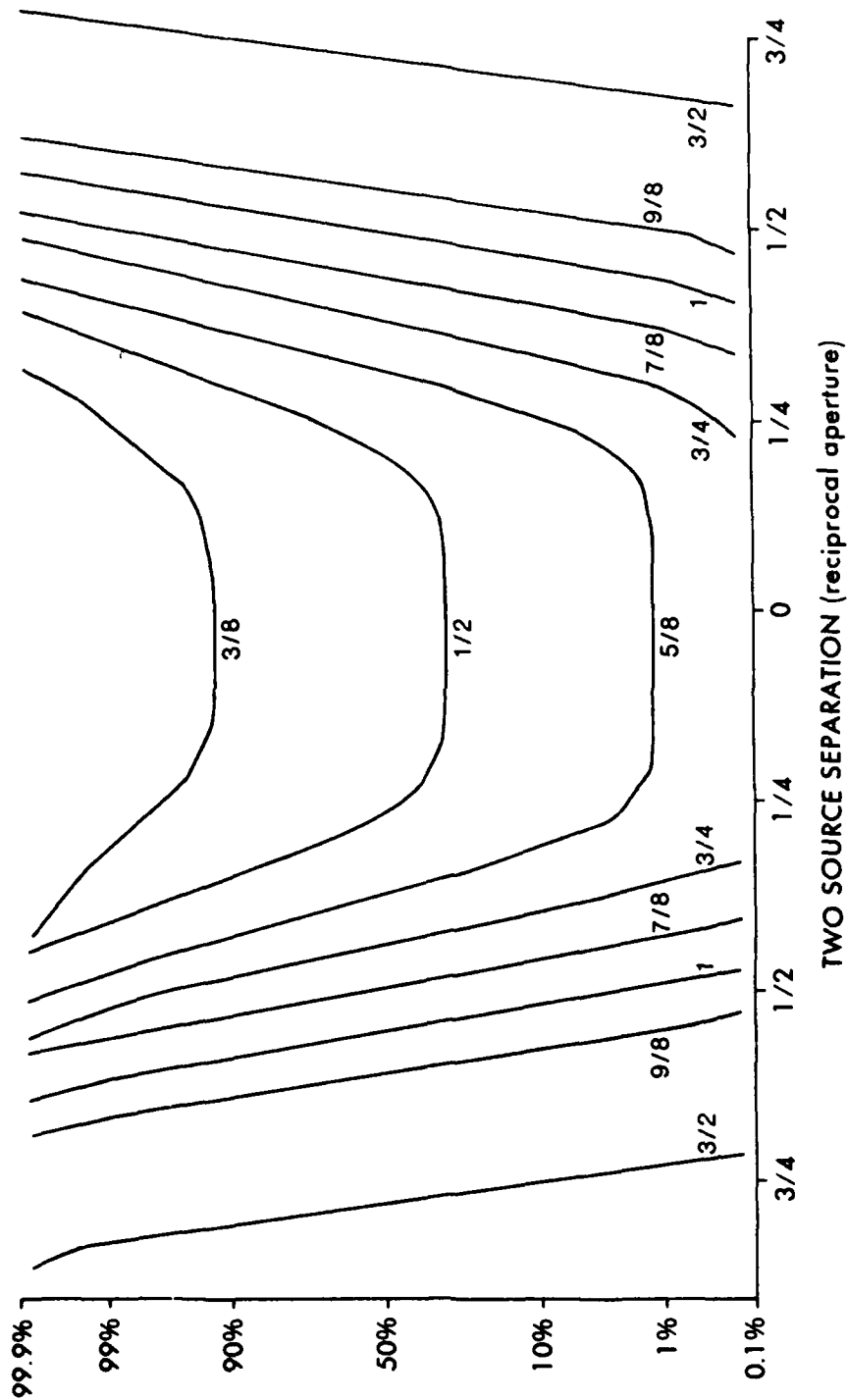


Fig. C4: Maximum Entropy Method

Probability of two source bearing estimation; the parameter is source separation measured in $1/\text{aperture}$.

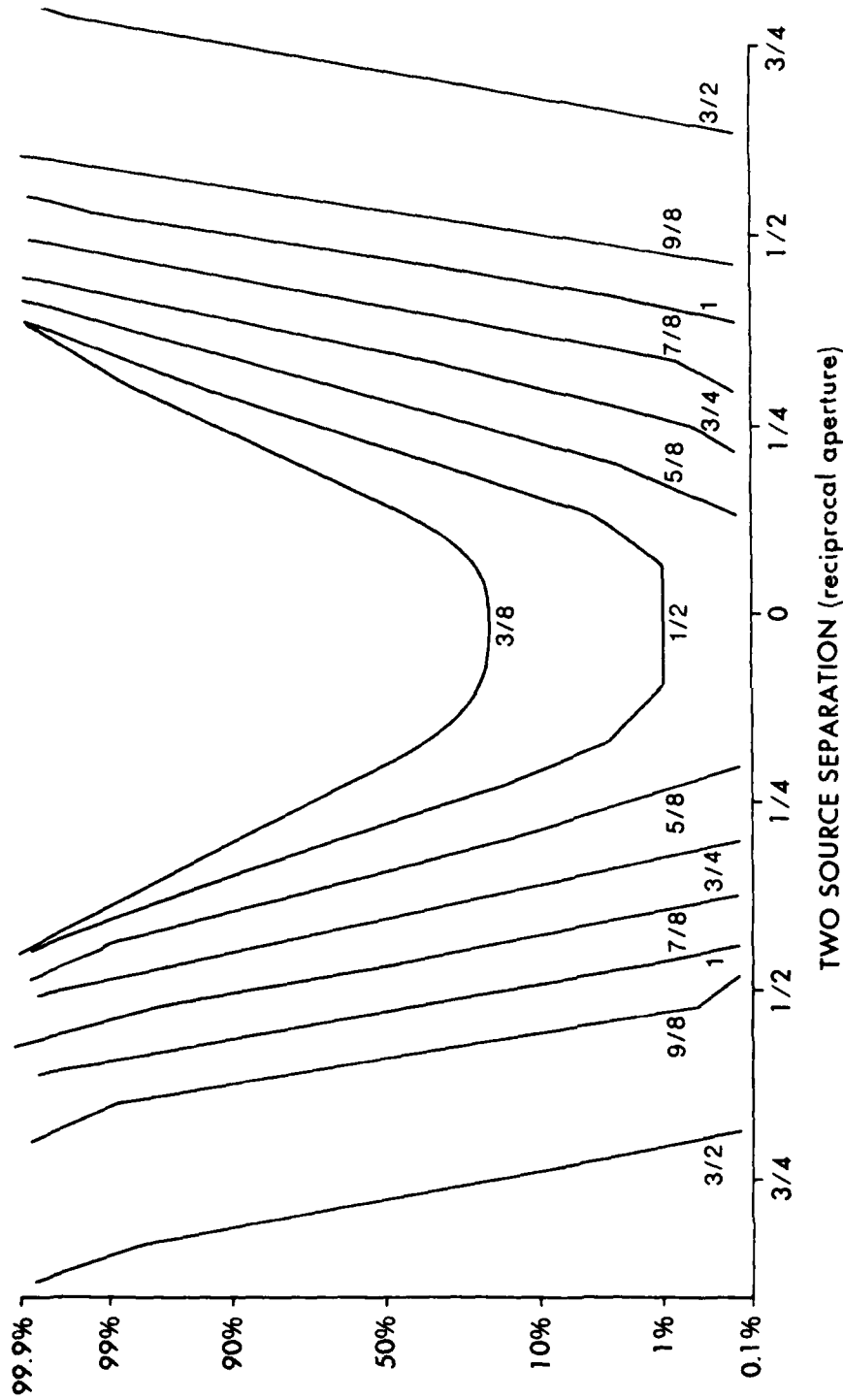


Fig. C5: Optimal Eigenvector Method

Probability of two source bearing estimation; the parameter is source separation measured in $1/\text{aperture}$.

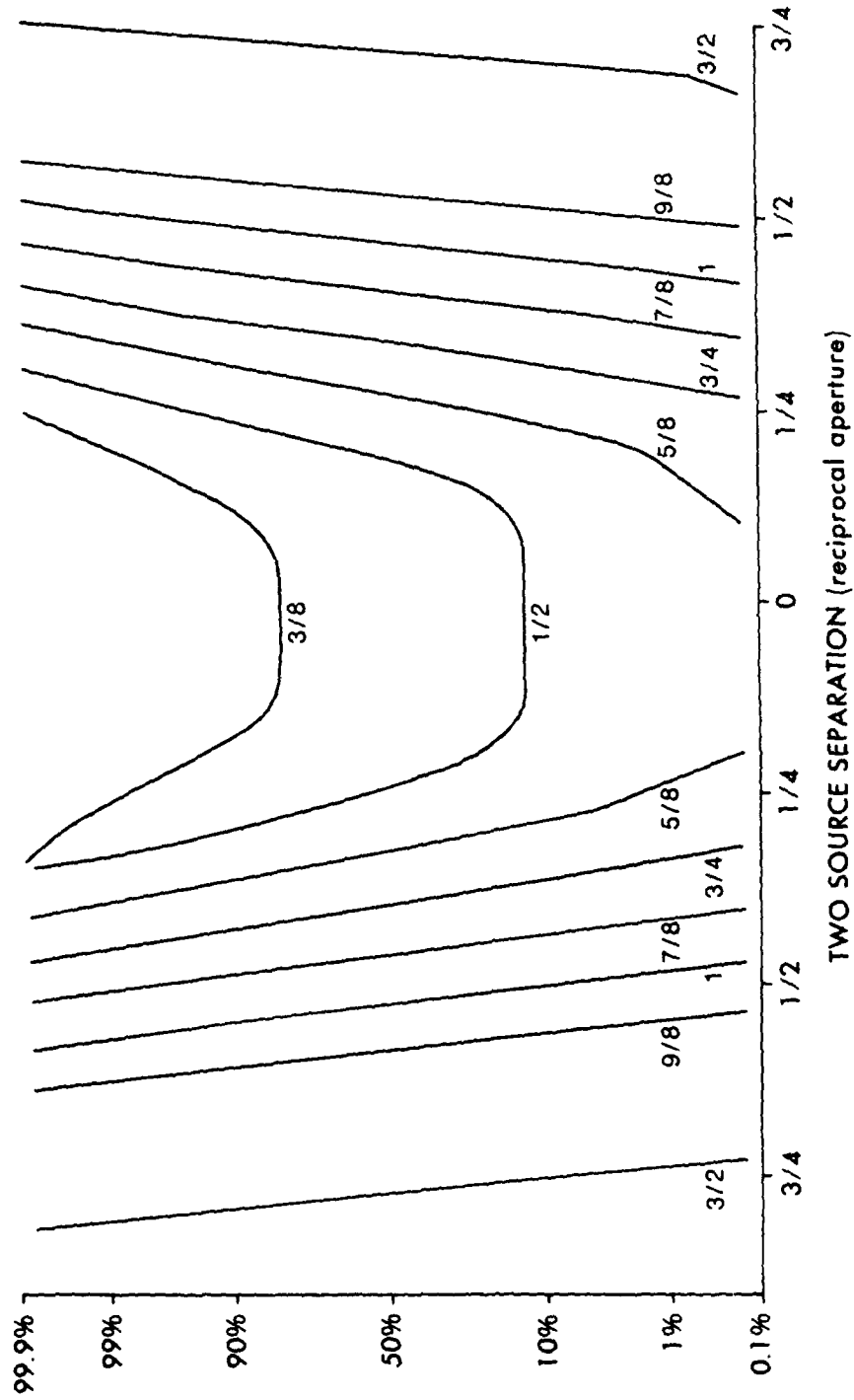


Fig. C6: Johnson Eigenvector Method

Probability of two source bearing estimation; the parameter is source separation measured in $1/\text{aperture}$.

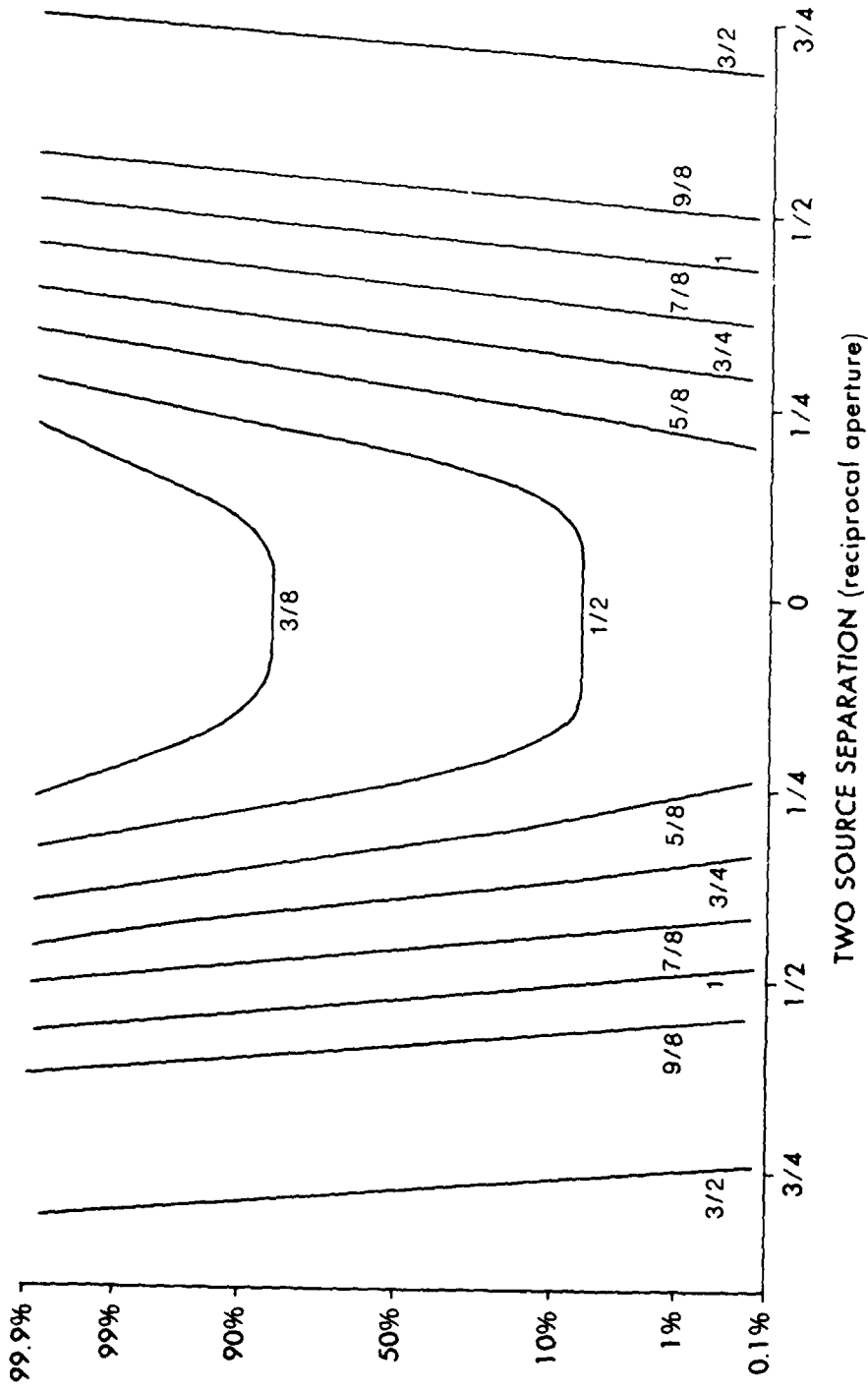


Fig. C7: Schmidt Eigenvector Method

Probability of two source bearing estimation; the parameter is source separation measured in $1/\text{aperture}$.

KEYWORDS

ACCURACY OF BEARING ESTIMATION

BLACKMAN-TUKEY METHOD

CAPON METHOD

CONVENTIONAL BEAMFORMING

DETECTION PROBABILITY

HIGH-RESOLUTION BEAMFORMING

JOHNSON EIGENVECTOR METHOD

MAXIMUM ENTROPY METHOD

OPTIMAL EIGENVECTOR METHOD

ORTHOGONAL BEAMFORMING

RESOLUTION PROBABILITY

SCHMIDT EIGENVECTOR METHOD

WIENER METHOD

INITIAL DISTRIBUTION

	Copies		Copies
<u>MINISTRIES OF DEFENCE</u>		<u>SCNR FOR SACLANTCEN</u>	
JSPHQ Belgium	2	SCNR Belgium	1
DND Canada	10	SCNR Canada	1
CHOD Denmark	8	SCNR Denmark	1
MOD France	8	SCNR Germany	1
MOD Germany	15	SCNR Greece	1
MOD Greece	1	SCNR Italy	1
MOD Italy	10	SCNR Netherlands	1
MOD Netherlands	12	SCNR Norway	1
CHOD Norway	10	SCNR Portugal	1
MOD Portugal	2	SCNR Turkey	1
MOD Spain	2	SCNR U.K.	1
MOD Turkey	5	SCNR U.S.	1
MOD U.K.	20	SEC GEN Rep. SCNR	1
SECDEF U.S.	68	NAMILCOM Rep. SCNR	1
<u>NATO AUTHORITIES</u>		<u>NATIONAL LIAISON OFFICERS</u>	
Defense Planning Committee	1	NLO Canada	1
NAMILCOM	2	NLO Denmark	1
SACLANT	10	NLO Germany	1
SACLANTREFUR	1	NLO Italy	1
CINWESTLANT/COMOCEANLANT	1	NLO U.K.	1
COMSTRIKELANT	1	NLO U.S.	1
COMIBERLANT	1		
CINCEASTLANT	1	<u>NLR TO SACLANT</u>	
COMSUBACLANT	1	NLR Belgium	1
COMMAIREASTLANT	1	NLR Canada	1
SACEUR	2	NLR Denmark	1
CINCNORTH	1	NLR Germany	1
CINCSOUTH	1	NLR Greece	1
COMNAVSOUTH	1	NLR Italy	1
COMSTRIKFORSOUTH	1	NLR Netherlands	1
COMEDCENT	1	NLR Norway	1
COMMARARMED	1	NLR Portugal	1
CINCHAN	3	NLR Turkey	1
		NLR UK	1
		Total initial distribution	248
		SACLANTCEN Library	10
		Stock	22
		Total number of copies	280

END

5-87

DTIC